REFINED SIEVERT INTEGRAL FOR THE CALCULATION OF DOSE DISTRIBUTION AROUND THE NEW BEBIG Co-60 HIGH DOSE RATE BRACHYTHERAPY SOURCE

This thesis is submitted to the University of Ghana, Legon in partial fulfillment of the requirement for the award of **MPHIL Medical Physics degree.**

BY

CASTROL DUMENYA

(10550675)

JULY, 2017

DECLARATION

"This thesis is a result of a research work undertaken by Castrol Dumenya in the department of medical physics, School of Nuclear and Allied Sciences, University of Ghana, under the supervision of Dr. Francis Hasford, Professor John H. Amuasi and Mr. Samuel Nii Adu Tagoe."

I hereby affirm that except for references which have been cited, this work is a product of my own research and it has not been presented in part or whole for any other degree in this University or elsewhere.

Sign……
Castrol Dumenya
(Student)
Date……...

Sign……
Dr Francis Hasford
(Principal Supervisor)
Date……..

Sign……
Prof. J. H. Amuasi
(Co-supervisor)
Date……

Sign……
Mr. Samuel N. A. Tagoe
(Co-supervisor)
Date……

ACKNOWLEDGEMENT

Over and over, again and again, God has shown his love and faithfulness to me by taking me through another educational level and my praise to Him would never end.

My second thanks and appreciation go to my magnificent supervisors Dr Francis Hasford and Prof John Humphrey Amuasi who have followed every detailed progress of this research work to a successful end, and have used their knowledgeable and scholarly experience to constructively criticise and correct my blunders. To the outstanding co-supervisor, Mr Samuel Nii Adu Tagoe, who birthed the idea for this research, helped in drawing the work plan, endowed apposite alternatives just for a solution to be obtained, I want to say a big thank you.

My overwhelming appreciation goes to Mr Evans Sasu, the indefatigable, incredundus and auriolus clinical medical physicist at the National Centre for Radiotherapy and Nuclear Medicine, KBTH; for his thorough on-site guide in obtaining results, making corrections where necessary in order to ensure accuracy.

My gratitude also goes to the brainy lecturers of the department of medical physics, School of Nuclear and Allied Sciences (SNAS), most especially Prof A. W. K. Kyere and Prof Cyril Schandorf for the concern shown in the progress of this research work.

I am also very thankful to Dr Raymond Edziah, Mr Michael Vowotor, Mr Charles Tetteh and Mrs Elizabeth Tetteh for their unquantifiable support at every step of the way.

To my good friends and colleagues, Kwesi Aane Koomson, Daniel Ackom, Nii Korley Corquaye, Belinda Buermle Asamanyuah, Eric Acomeah, Emmanuel K. Nyogbe, Philip Odonkor, Blessing Ayivi, Ms Shiela Victoria Gbormittah, I am grateful for the love shown during the period of this programme. To the formosus and exquisite Ms Mavis Yorm Aleawobu, I am deeply grateful for the love and support shown me throughout the period of the program.

To my relatives Mr Forgive Torwudzo and wife, Mrs Bless Nyamuame-Glover, Ms Felicia Nyamuame, Michael Nuwormegbe and my siblings, Believe, Blessing and Godsway Dumenya, your support has been immeasurable. Thanks for everything. God bless you all

DEDICATION

This research work is dedicated to my parents and heroes, Mr Ricky Seth Dumenya and Mrs Rebecca Dumenya, and my siblings for their lifetime support, wise counsels and prayers done on my behalf throughout my educational career.

TABLE OF CONTENTS

LIST OF FIGURES

LIST OF TABLES

APPENDICES

LIST OF ABBREVIATIONS AND SYMBOLS

AAPM	-	American association of physicists in medicine
DVH	-	Dose volume histograms
EBRT	-	External beam radiotherapy treatment
FFT	-	Fast Fourier transform
HDR	-	High dose rate
ICWG	-	Interstitial Collaborative Work
KERMA	-	Kinetic energy released in matter
LDR	-	Low dose rate
MDR	-	Medium dose rate
MC	-	Monte Carlo
OAR	-	Organs at risk
PTV	-	Planning target volume
GTV	-	Gross tumour volume
CTV	-	Clinical target volume
RTP	-	Radiotherapy practice
RTPS	-	Radiotherapy treatment planning system
TPS	-	Treatment planning system
TERMA	-	Total energy released in matter
CP	-	Control point

TG43	-	Task group 43
1D	-	One dimension
2D	-	Two dimension
3D	-	Three dimension
^{60}Co/Co-60	-	Cobalt 60
^{192}Ir	-	Iridium 192
ICRU	-	International Commission on Radiation Units and Measurement
ROI	-	Region of interest
POI	-	Points of interest
KBTH	-	Korle Bu Teaching Hospital
NCRNM	-	National Center for Radiotherapy and Nuclear Medicine
QA	-	Quality Assurance
QC	-	Quality control
TLD	-	Thermoluminiscent dosimeter
IFT	-	Inverse Fourier tansform
ISL	-	Inverse square law
CT	-	Computerised tommography
MRI	-	Magnetic Resonance Imaging

ABSTRACT

A very good reason why calculation of dose distribution is important is that it is essential to plan and replicate the treatment prior to the actual delivery of the radiation dose to the tumour. In modern radiation therapy, computer software is used for performing treatment planning. Different algorithms are employed at every stage of treatment including dose calculation algorithms. The dose calculation used for the HDRplus TPS is the TG43 formalism and just like every other TPS, the HDRplus, version 3.0.5, may produce erroneous results, (Daskalov, 1998) and it is essential to eliminate or reduce these errors through a quality control procedure of manual calculations. This will further improve treatment outcomes since TPS approximations are used in executing treatment. The Sievert integral algorithm is commonly used in radiotherapy treatment planning systems (RTPS) for evaluation of dose around brachytherapy sources and it is an established tool for ^{125}I, ^{169}Yb, ^{137}Cs and ^{192}Ir (Bhola *et al*, 2012). The source under consideration is the new model (Co0.A86) of the BEBIG ^{60}Co HDR source, hence the need to establish the Sievert as a valid tool for quality control for the output of the TG43 based HDRplus TPS using this source. From the results obtained, the percentage deviation range of the dose output from the Sievert integral in comparison to that of the output from the TPS is 0.03 – 10.51% with a mean of 3.13% for angle range of $0^{o} < \theta < 70^{o}$. The Sievert integral breaks down at respectively large angles and therefore neglecting the breaking point oblique direction, i.e. $\theta \geq 60^{o}$, the range becomes 0.03 – 5.63% with a mean value of 2.55% for the angle range of $0^{o} < \theta < 48^{o}$. Following the ICRU report 24 that percentage deviation of dose values calculated should not exceed ±5% of the true value, the Sievert integral has proven to be a valid tool for quality control of the HDRplus using the range with less error.

CHAPTER ONE

INTRODUCTION

1.1 BACKGROUND

In Ghana, cancer forms 16% of the top 50 causes of death and two-thirds of cancer deaths occur in developing countries (Health Profile: Ghana, http://www.worldlifeexpectancy.com/country-health-profile/ghana.html). This has resulted in a large number of cancer related research. Different modes of cancer treatment have been adopted in health facilities in Ghana and these include surgery, chemotherapy and radiotherapy.

Radiotherapy, radiation oncology or therapeutic radiology, is one of the key modalities used in the management of malignant diseases (cancer). In dissimilarity to other medical areas that rely mainly on the clinical expertise and experience of medical officers, radiotherapy, with its use of ionizing radiation in the treatment of cancer, relies heavily on modern technology and the collective efforts of numerous professionals, including medical physicists. The coordinated team approach for treating cancers greatly impacts the treatment outcome (Podgorsak, 2005). Radiotherapy involves the use of high energy ionizing radiation in the treatment of tumour cells. It is classified into two categories; external beam radiation therapy (EBRT) and brachytherapy. For the purpose of this research, much emphasis will be laid on brachytherapy.

Brachytherapy, sometimes referred to as curietherapy, is used to describe the short distance treatment of cancer with radiation from small, encapsulated radionuclide sources (Podgorsak, 2005). This method of treatment is used to deliver radiation to localised tumors by interstitial, intracavitary, or surface application (Kyeremeh *et al*, 2012).

Intracavitary treatments are at all times short-term, whereas interstitial treatments may either be short-term or permanent. Intracavitary brachytherapy involves placing sources into cavities proximate to the tumour volume, while interstitial brachytherapy deals with implanting sources surgically within the tumour volume. In temporary applications, dose is delivered over a short time interval compared with the half-life value of the radionuclide and the encapsulated radioactive source is taken off from the patient once the expected dosage is attained. In the case of permanent applications, the delivered dose lasts over the lifespan of the encapsulated source till it is completely decayed. Depending on the treatment duration, brachytherapy could be termed as low dose-rate, LDR (between 0.4 and 2 Gy/h), medium dose-rate, MDR (between 2 Gy/h and 12 Gy/h) and high dose-rate, HDR (greater than 12 Gy/h). (Acquah, 2011)

Between 10 and 20% of all radiotherapy cases are treated using brachytherapy in typical radiotherapy departments. Its great value is attributed in part to the delivery of lethal dose to target organs with minimal dose reaching the nearby healthy tissues (Khan, 1994). The main advantage of this technique is the high conformal radiation dose delivered to the malignant tumour volume and sparing of the healthy organs or tissues at risk due to the inverse square law on the dose distribution around the radiation source thereby producing improved localized dose to the target region of interest (ROI) as compared with external beam radiotherapy. The setback is that

brachytherapy can only be used in cases in which the tumour is well localized and relatively small (IAEA, 2007; Acquah, 2011).

Dose calculation algorithms are the most essential software components in a computerized treatment planning system (TPS). These modules are accountable for the correct illustration of dose in the patient, and could be connected to treatment time, dwell times of source and localization of brachytherapy sources.

The feats attained in the provision of radiotherapy modality of cancer treatment may decline if not harmonized using arduous dose calculation models and algorithms (Papanikolaou & Stathakis, 2009). Basically, it's because the efficiency and superiority of any TPS largely depends on the sort of algorithms employed at each diverse phase of the process of planning. Based on manufacturer preferences, several types of dose calculation algorithms are used in modern TPS, but the best dose computational algorithm should be easy to use with its speed and accuracy well put together (Kyeremeh *et al*, 2012). The quality of the dose distribution representation of a good algorithm depends strongly on the data or the parameters used by the algorithm (Oguchi *et al* 2005). The concurrence between the calculated and delivered dose is of great importance in radiotherapy since the accuracy of the absorbed dose based on prescription determines the clinical outcome (Oelkfe & Scholz, 2006).

There is a dual function of dose calculation algorithms in the practice of radiotherapy:

i. for plan enhancement in the process of treatment planning
ii. for nostalgic comparison of the relationship between the available treatment parameters and clinical output.

It outlines two conjointly incompatible objectives of the particular dose calculation algorithm under consideration. To start with, the dose calculation algorithm has to be

expeditious so as to facilitate the treatment planning process in medically satisfactory time frame and secondly the outcome of the dose calculation has to be adequately accurate so that the establishment of the relationship between delivered dose and the clinical outcome remains consistent and significant. This has called for more review into the subject of dose calculation (Oelkfe & Scholz, 2006).

There are different dose calculation algorithms that are used in brachytherapy. These are Monte Carlo, Superposition-Convolution model, Sievert Integral model and the latest being the AAPM TG43 formalism.

The Sievert integral is a substitute to experimental or other dose calculation algorithms. This method basically involves dividing a line source into small elementary sources and applying the inverse square law and filtration corrections to each. It is an indispensable tool for dose rate calculations around brachytherapy sources, combining simplicity with equitable computational times, requires limited input data and is computationally efficient. This gives the Sievert Integral an advantage over the Monte Carlo (MC) technique which requires large volume of input data and high computational time. The limitation of the Sievert integral not being accurate in predicting dose rate distributions around low energy isotopes will not be a problem in this research study because the source in this case is ^{60}Co (Nani *et al*, 2009).

Various forms of the Sievert Integral algorithm have been used for over the past nine decades. The Sievert Integral could be modified to correct for photon attenuation in tissue. The classical Sievert Integral model lumps the primary beam and scattered beam together and this takes care of the effect of the inverse square law.

Modifications in the basic model of the Sievert integrals increase the accuracy significantly, nevertheless there are still discrepancies between the output from the Sievert integral and other dose calculation algorithms (Nani *et al*, 2009). This study seeks to obtain the dose distributions around the new BEBIG ^{60}Co source based on the version of the Sievert integral where the source strength is specified in air kerma (Khan, 2010). The results will then be compared to the output of the TG43 based HDRplus TPS which is used at National Center for Radiotherapy and Nuclear Medicine, Korle Bu Teaching Hospital (NCRNM, KBTH).

1.2 STATEMENT OF RESEARCH PROBLEM

As part of quality assurance (QA) procedures for HDR brachytherapy, it is required to perform some manual calculations to estimate doses at specific points called control points (CPs) around the brachytherapy source. This is used to validate the output of the TPS since dosimetry using a TPS may sometimes produce erroneous results (Daskalov *et al*, 1998) especially at proximal distances as has been recorded for ^{192}Ir sources (Cohen *et al*, 2000). Sievert integral as stated earlier, is one of the methods which can be used to calculate the dose distributions around a brachytherapy source. There is therefore a need for validation of this method for the HDRplus TPS in use for dose distribution determination for the new BEBIG ^{60}Co HDR Multisource afterloader brachytherapy machine (Eckert & Ziegler BEBIG GmbH, Germany) at the NCRNM, KBTH. The HDRplus TPS runs on TG43 algorithm and the afterloader machine uses ^{60}Co with code name Co0.A86.

1.3 OBJECTIVE OF THE STUDY

The goal of this study is to identify a robust way of calculating the dose distribution around the BEBIG Multisource Afterloading brachytherapy source (Co-60) and establish the efficacy of the method (Sievert integral) by comparison with the output of the HDRplus.

1.4 SPECIFIC OBJECTIVES

a) To obtain a treatment plan for the study using the HDRplus.

b) To digitally obtain doses at different locations in a *x-y* plane, called (CPs) and the corresponding dwell-times of the ^{60}Co source.

c) To obtain the Sievert integral values for the various angles of the CPs with respect to the source positions.

d) To write a MATLAB program to compute the dose value for the various input data to be fed into the program in order to obtain values for each CP.

e) To make a statistical analysis, through graphical representation of results obtained from calculation and the TPS and find the percentage deviation of Sievert integral doses from the HDRplus doses.

1.5 SCOPE OF THE STUDY

The study involves obtaining a treatment plan and positioning digitized sources in a universal applicator at different locations on the vertical axis of a 2D-plane. A prescribed dose of 2 Gy will be delivered, and dose measurements taken at twelve CPs. For each source dwell positions, the dose will be normalised to a distance of 1 cm. The resultant dwell-times, which will automatically be calculated by the

HDRplus, will equally be used in obtaining the dose values from the Sievert integral procedure. Other required parameters will be inputted into the dose calculation formalism under study and the results will then be analysed.

1.6 JUSTIFICATION AND RELEVANCE OF THE STUDY

The Sievert integral has been used for estimating the dose distribution around ^{192}Ir brachytherapy source, and the outcome was compared with the Monte Carlo technique and uncertainties in a range of 3.5 – 5.8% were observed along the axis of the brachytherapy source (Nani *et al*, 2009). It is therefore prudent for this study to be performed on the new BEBIG ^{60}Co source and to compare the results with the TG43 formalism which is the most widely adopted dose calculation formalism in most radiotherapy centres, including the NCRNM.

The HDRplus, version 3.0.5, just like every other TPS may produce erroneous results, as established by other research work, (Daskalov, 1998) and it is essential to eliminate or reduce these errors through a quality control procedure of manual calculations. This will further improve treatment outcomes since TPS approximations are used in executing treatment.

1.7 ORGANISATION OF THESIS

Chapter one deals with the background of the study, the problem statement, objectives, justification and relevance of the work, scope and limitation. Chapter two contains literature review relevant to the research work. Chapter three describes the research materials and methods used to conduct the study. Chapter four outlines the

results obtained and subsequent discussions on the findings while chapter five gives the conclusion, recommendations and suggestions for further studies.

CHAPTER TWO

LITERATURE REVIEW

2.1 INTRODUCTION

This chapter discusses in-depth literature on the various dose calculation models with much emphasis on the TG43 formalism which is the universally accepted dose calculation model, the fast Fourier transform (FFT) or convolution formalism and MC formalism.

Treatment of cancer with radiation (radiotherapy) is carried out with the ultimate goal of delivering the prescribed dose to a tumour precisely and simultaneously minimising the dose reaching critical organs. The key element of a treatment planning system (TPS) is the calculation of dose and the accuracy of the calculations which directly has bearing on the quality of a treatment while its speed greatly affects the clinical flow.

2.2 DOSE CALCULATION

A very good reason why calculation of dose distribution is important is that it is essential to plan and replicate the treatment prior to the actual delivery of the radiation dose to the tumour. Since the goal is to kill the tumour with radiation from a sealed source placed in a patient (brachytherapy) or from a distance (teletherapy), a precise dose needs to be absorbed by the tumour and this can only be guaranteed by performing dose distribution calculation through the management of radiation beams

which are characterised by various parameters in the treatment machine used in the delivery of radiation. This procedure is referred to as treatment planning.

Computer software is used for performing treatment planning in 21st century radiotherapy. This is done by making use of patient's images to recognize and locate the internal body structures together with the parameters of the machine to simulate the actual treatment. The simulation results produces the calculated doses for the target as well as those for the organs at risk (OAR) and other regions of interest (ROI). The accuracy of the calculation of dose distribution and the high level quality assurance programme carried out on the TPS is essential to make sure that dose delivery to the tumour is equal to or close to 100% of the calculated dose (Lu, 2013).

The total accumulated energy of ionising radiation absorbed by a unit mass of body tissues defines the radiation dose. Therefore, dose calculation is the computation of the energy absorbed by the media at any points that radiation beam particles pass or may not pass through, where various physical processes take place due to interactions, such as Compton's scattering, between the beam particles and the media (Lu, 2013). At specific points of interest (POI), the accumulated dose is a contribution from the interaction of incident beam with points in the patient, and scattered radiation beam. A very good dose calculation algorithm compromises between large amounts of data storage and accuracy, and lengthy calculations. This compromise will only be meaningful if calculations are carried out with speed and accuracy (Lu 2013; Kyeremeh, 2011)

2.3 EVOLUTION OF DOSE CALCULATION ALGORITHMS AND DOSIMETRIC SYSTEMS

Developments in the field of nuclear and particle physics and computer science have seen the rapid evolution of dose calculation algorithm since the middle part of the twentieth century. This has led to an enhanced understanding of the physical processes involved in the interaction of radiation with a medium and has enabled simulation and calculation of doses for complex system within a short of period of time (Lu, 2013)

Dosimetric systems and techniques have gone through phases of change for a few decades. A typical illustration is the idea or assumption that was made that a uniform distribution of sources on a surface applicator or for a single planar interstitial implant would result in a uniform dose distribution at the treating distance of usually 0.5 cm or 1.0 cm (Wickham and Degrais, 1910, Baltas *et al*,2007). This opinion was valid in clinical practice until the latter years of 1920s. As at the 1930s it became unambiguously proven that this was untrue and that a non-uniform placement of brachytherapy seeds resulted in an even distribution of dose. This laid the foundation for the formation of the Manchester System of Paterson and Parker, which came into being in the 1930s (Meredith, 1947; Baltas *et al*, 2007). The outcome from theoretical findings on the exposure rate distribution quantified in roentgens around brachytherapy seeds of less complex geometrical feature, such as line, annulus, sphere and cylinder, aided the formulation of rules for the system. More research had been done about line sources at an earlier period and the Sievert integral being popular by then (Sievert, 1921; Baltas *et al*, 2007). The Manchester System was commonly used till the 1970s before the inception of computerised treatment planning, in addition to a system known as the Quimby system, birthed in the early 1920s and became the

system adopted and used in the United States. These two methods were then taken to be the standard of brachytherapy dosimetry for subsequent years (Baltas *et al*, 2007).

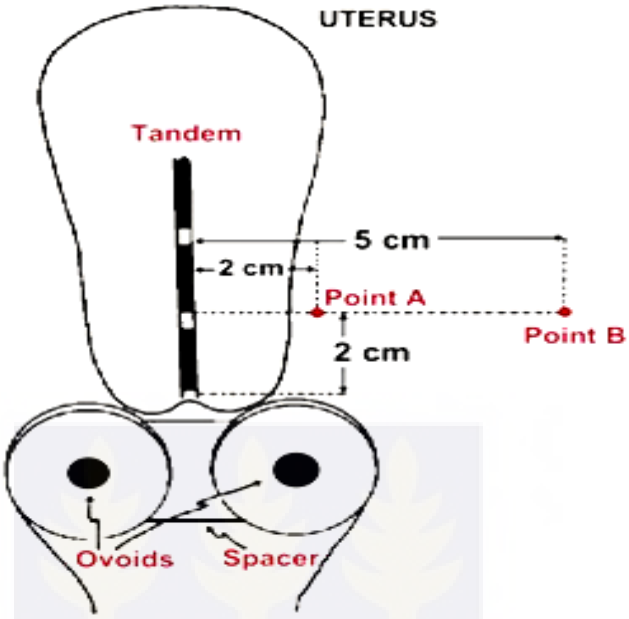

Figure 2. 1: The Manchester system used in the calculation of doses at two points A and B (Khan, 2010)

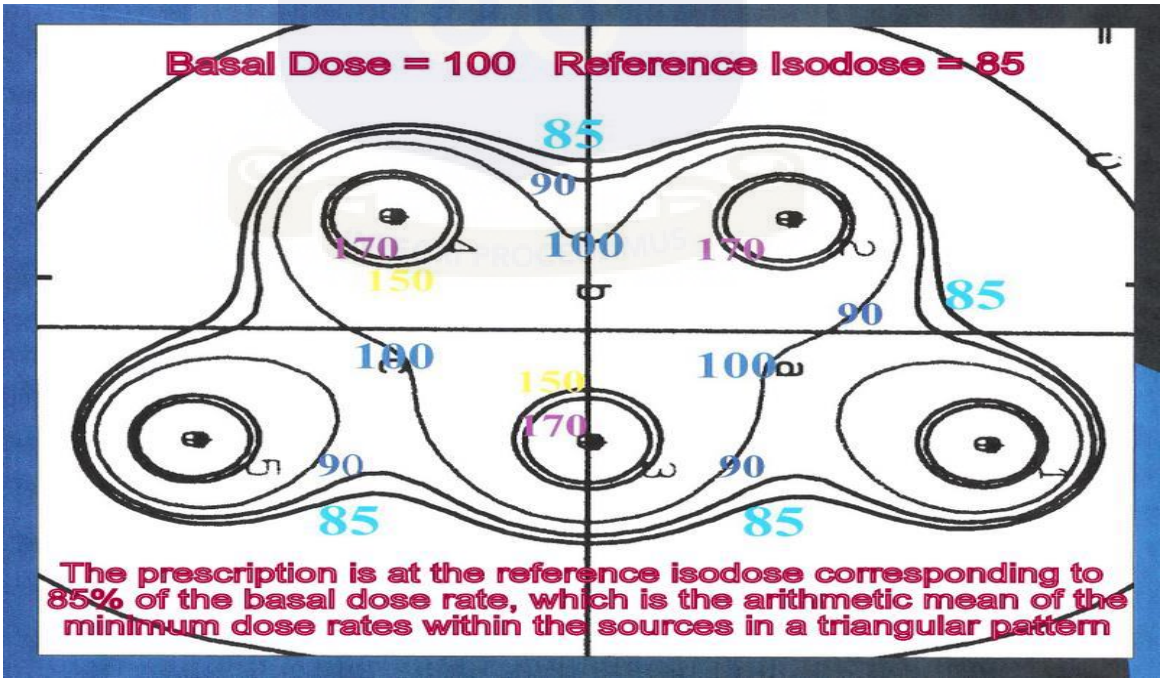

Figure 2. 2: Paris System prescription for breast implant

Planning of an interstitial implant for both systems entailed the determination of the area or volume of a target region and then consulting a table or graph for the required total source strength, measured in milligram-hours, per unit peripheral dose rate. The Manchester system (method clearly indicated in fig 2.1) sought to deliver ±10% of the prescribed dose throughout the region implant while the Quimby system sought to deliver a uniform distribution of source strength of equal linear activity and accepted the hot spots in the central region of the implant (Meredith, 1947; Baltas *et al*,2007).

At a later time, the Paris system (method of source arrangement displayed in fig 2.2) was developed but was modelled for use with Ir-192 wires. Its dosimetry is based on the measurement of the dose rate at the central part of the volume being treated, which is called the basal dose rate. Its calculation is from the dwell position of the wires in the central plane and is the least dose rate between two wires while taking note that the correlation between the basal dose and the layout of the Ir-192 wires is very essential.

International approvals (ICRU report 58, 1997) have been introduced for dose and volume requirement in interstitial brachytherapy which replace the earlier concepts and terminology such that in place of volumes and planes, we have the following; gross tumour volume (GTV), clinical target volume (CTV), planning target volume (PTV), treated volume and central plane.

To give a detailed description of the dose distribution, the quantities used are: prescribed dose, minimum target dose, mean central dose, high dose volumes, and low dose volumes.

Other systems have equally been introduced, for example, the dose-volume histogram (DVH). Theoretical evaluations pertaining to the distribution of dose around radium

brachytherapy seeds began in 1916, about five years before the conception and publication of Sievert integral method for linear radium brachytherapy seeds and were sustained through many decades with different sources and modifications made to the integral to suit specific expected outcomes, alongside other modern techniques. Experimental measurements were also undertaken with rather rare options to imitate the neighbouring organs for an actual patient. Those used were rabbit and rat muscle and butter. The basic standard of the use of the butter phantom was that by creating slices in the butter, and decolourizing it using gamma rays from radium would efficiently produce isodose curves.

For other forms of brachytherapy, such as the intracavitary gynaecological uses for either the cervix uteri or the corpus uteri, and the endometrium, dosimetry systems were also developed. Also, doses could be calculated from first principles; thus calculation of dose rate around point sources, line sources or encapsulated cylindrical source. Some advanced methods are two dimensional formalism, three dimensional dose calculation-convolution technique, Monte-Carlo technique, Sievert integral technique, etc. (Lu 2013; Kyeremeh, 2011).

2.4 DOSE-RATE CALCULATION AROUND A POINT AND LINE SOURCE

A point source describes the least uncomplicated situation to calculate in the quest to create an approximate calculation algorithm. For point sources, radiations from charged particles are neglected and consideration is made only of photons. This is so because commercial sources are encapsulated and therefore the encapsulation scatters and slows down the electrons in that most do not leave the source capsule and for the

few that escape, their range in tissue outside is much smaller than 5 mm and therefore assume not to contribute at clinical prescription distances. Considering a sample of radioactive material whose largest dimension is smaller than 0.01 mm, all the atoms are considered to be located at a single point. The resultant dose rate in a small volume, ***dv***, of tissue located at a distance, ***r***, from the source (in vacuum, such that there is no scatter) and that a photon is emitted at every time, ***t***, with energy, ***E***, will be given by the product of time rate of emission of the photon (activity), the probability of the photon hitting ***dv***, the probability of photon of energy ***E***, which imparts and interacts with the small volume and the average amount of energy $\boldsymbol{dE}_{\text{abs}}$ that is absorbed in ***dv*** all divided by the mass, ***m***, of the small volume. The dose rate is then expressed as energy/mass/time, explicitly expressed as (Daskalov *et al*, 1998)

$$\dot{D}(r) = A \times P(r, dv) \times P(E, dv) \times \frac{dE_{abs}}{m} \qquad (2.1)$$

Where,

dv = small volume of tissue

r = distance from source centre

E = energy of source (intrinsic)

A = activity

P(r,dv) = probability of photon hitting dv at a distance r from source center

P(E,dv) = probability of photons with energy E which strikes the volume dv

$\boldsymbol{dE_{abs}}$ = average amount of energy absorbed in dv

Line sources are considered as an extremely thin source of active length, L, of radioactive material and in such instances, the direction and distance with respect to

the centre of the line is considered but symmetry still remains (Daskalov *et al*, 2000). For a line source, the dose rate at any point in the plane is derived by defining the activity per unit length of the source and integrating the point source expression.

$$\dot{D}(r) = \frac{f_{med} A \Gamma B(r)}{r^2} \qquad (2.2)$$

Considering the entire length of the source, the final result is calculated using the relation

$$\dot{D}(r) = \frac{f_{med} A \Gamma B(r)}{L} \int_{-\frac{1}{2}}^{+\frac{1}{2}} \frac{dL}{r^2} = \frac{f_{med} A \Gamma B(r)}{Lr \sin\theta} \beta \qquad (2.3)$$

The length, ***L***, is the active length of the source and $\beta = \theta_2 - \theta_1$ is the angle subtended by the source when viewed by the source when viewed from a point.

For encapsulated sources used in clinical practice, the active source region in the cylindrical encapsulated source is divided into smaller points and contributions from these points are determined separately using equation (2.1) and the results are then added up. The encapsulation reduces the dose rate by an amount dependent on the path length through the encapsulation. Since the path length through the encapsulation from each point source is not the same, the individual contributions to dose rate varies in all directions and hence the solution to this encapsulated line source has been proposed by the Sievert integral. **(**Neuenschwander *et al* 1995*;* Miften *et al* 1999)

2.5 TWO-DIMENSIONAL DOSE CALCULATION FORMALISM

The AAPM in 1988 formed a Task Group (TG43) to address some outstanding issues emanating from brachytherapy source dosimetry formalisms. The resultant dose calculation model proposed by the Task Group 43 resulted from the publication of the

ICWG in 1995 and has gained universal recognition and adoption (Nani *et al*, 2009). The proposed 2D dose distribution calculation formalism based on the TG43 is confined to quantities that are measurable and dissociates a few interdependent quantities and also includes new constants dedicated to the various sources (Meli *et al*, 1988). 2D dose distribution calculations around brachytherapy seeds have been made feasible with this protocol and have resulted in absolute dose rate change by 17% with respect to traditionally used treatment planning data at that time (Ravinder *et al*, 1994; Kline and Earle, 2007; ICWG, 1990). The newly proposed TG43 formalism demands input data comprising dose-rates obtained from a real brachytherapy seed placed in a tissue equivalent phantom and depends on the particular source, the source geometry and construction in addition to primary photon spectrum and medium unlike the conventional method which adopts exposure rate constant and tissue attenuation factors (Ling *et al* 1985; Schell *et al* 1987; Weaver *et al* 1989; Nath *et al* 1995).

A pure brachytherapy seed manifests significant anisotropy and therefore it is difficult to perfectly obtain dose distribution from photon fluence and free space. The TG43 model lacks this basic setback through an undeviating implementation of measured or measurable dose distribution a source in a homogeneous medium (Nath *et al*, 1995). The TG43 model also puts into restrictive consideration cylindrical symmetric sources. For such sources, the dose distribution is in 2D and is best illustrated in terms of polar coordinates with its origin located at the centre of the active source.

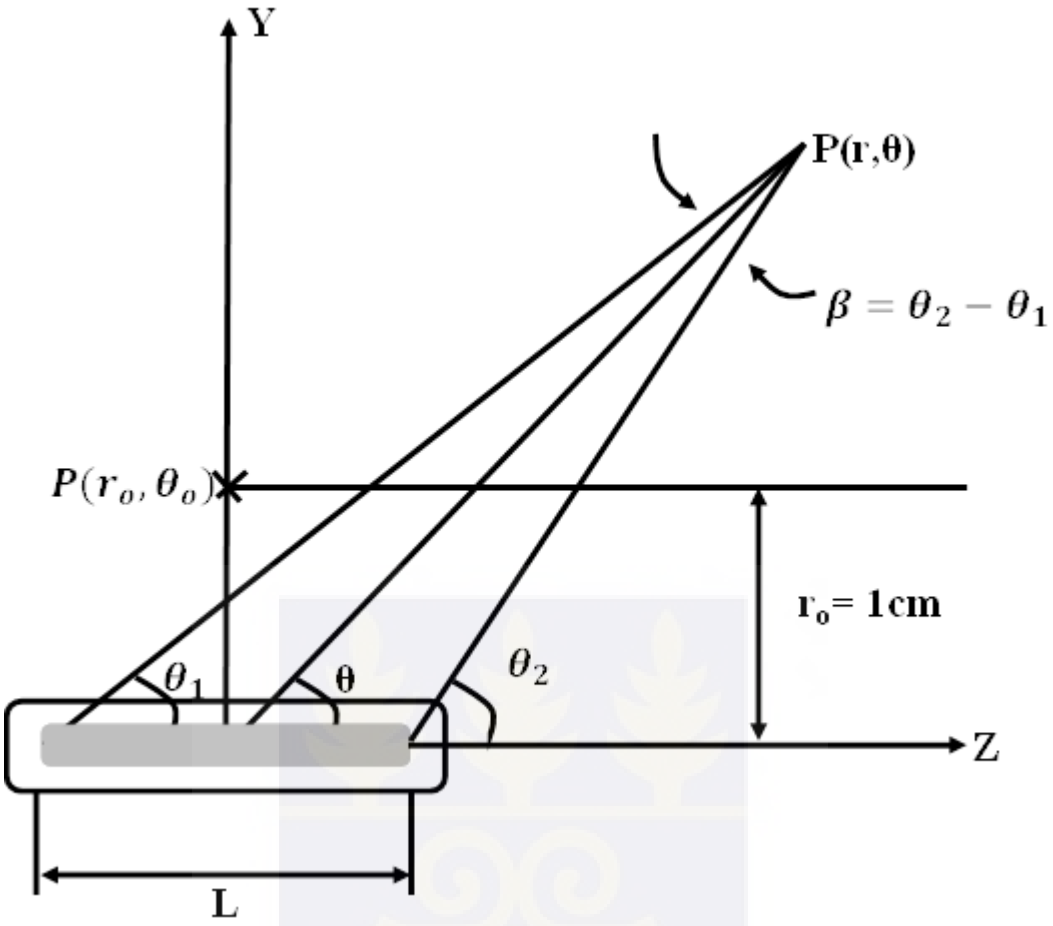

Figure 2.3: Geometry used in the calculation of dose distribution near a linear source based

Based on the TG43, the dose rate at a specified point *(r,θ)* in a medium for the source of strength, S_k, is given by

$$\dot{D}(r,\theta) = S_k \Lambda \frac{G(r,\theta)}{G_o(r_o,\theta_o)} F(r,\theta) g(r) \qquad (2.4)$$

Where

r = distance (cm) from the origin to the point of interest, P

θ = angle between the direction of radius vector r and the long axis of the source

θ_o = source transverse plane and is equal to π/2 radians

S_k = air kerma strength of the source $mGym^2h^{-1}$

Λ = dose rate constant in water

$G(r,\theta)$ = geometry function

$g(r,\theta)$ = radial dose function

$F(r,\theta)$ = anisotropy function

The equation (2.4) is used for both point and line source approximations to expedite the dose computation process. All parameters in the equation are referenced to the same single points and the product ΛS_k is the dose rate in water at the reference position (r_o,θ_o). The reference point is situated at a distance 1cm along the perpendicular bisector (transverse axis) of the source as shown in fig.2. , i.e. $r_o = 1cm$ and $\theta_o = \pi/2$

Air kerma strength, S_k, as a measure of brachytherapy source strength is specified in terms of brachytherapy source at a point along the transverse axis of the source in free space is defined as the product of air kerma rate at a calibration distance $\dot{K}(d)$ and the square of distance d.

$$S_k = \dot{K}(d)d^2 \qquad (2.5)$$

S_k is the measure of the absolute amount of radionuclide available. Its source calibration unit U is equal to $cGycm^2/hr$ by definition. (Kline and Earle, 2007; Nath et al 1995)

The dose rate constant (Λ) expresses the dose rate to water at a distance of 1cm on the transverse axis as a unit kerma strength source in a water phantom. It is given as

$$\Lambda = \frac{\dot{D}(r,\theta)}{S_k} \qquad (2.6)$$

The dose rate constant is determined once for each of the manufacturer's source using Monte Carlo modelling plus experimental measurements usually with TLDs (Nani *et al* 2009; ICWG 1990; Ling *et al* 1985; Schell *et al* 1987). Errors are present in both procedures and hence results are averaged to yield a consensus value for Λ (ICWG, 1990). As a result of the effect of the distribution of the activity within the source encapsulation, self-filtration within the source and scattering in water around the source, the evaluation of the dose rate presents a measurement uncertainty (Nani *et al*, 2009).

The parameter $G(r,\theta)$ represents the geometric function that gives detailed information for the geometric fall off of the photon fluence with respect to the distance from the source and, it is dependent on the distribution of radioactivity inside the material. The geometry factor suppresses the influence of inverse square law on the dose distribution around the source. There is a large dose rate gradient around interstitial brachytherapy sources and this makes it difficult to estimate accurate dose rate at distances less than 5 mm from the source. Also, the large variation in dose rate that emanates from the inverse square law makes accurate interpolation of intermediate dose rate values very difficult. Therefore, suppressing the inverse square law effects and extrapolating to small distances from the dose rate profile measurement at 5 mm and 10 mm as well as interpolating between scantily distributed measured values increases accuracy. From the TG43 model, there are two geometric functions that are considered for both point and line sources. (Nani *et al*, 2009; Weaver *et al*, 1989; Nath *et al* 1995)

Point source is given as $G_p(r,\theta) = {}^{1}/_{r^2}$ (2.7)

Line source is given as $G_l(r,\theta) = \frac{\beta}{Lr\sin\theta}, \theta \neq 0$ (2.8)

The radial dose function, *g(r)* accounts for the effect of absorption and scatter in the medium along the transverse axis of the source. It is defined as

$$g(r) = \frac{\dot{D}(r,\theta_o)G(r_o,\theta_o)}{\dot{D}(r_o,\theta_o)G(r,\theta_o)} \qquad (2.9)$$

The fall off of those rates in the direction along the transverse axis due to absorption and scattering in the medium is defined by the function, *g(r)*. It is modelled by filtration of photons by source materials and encapsulation (Nath *et al*, 1995; Nani *et al*, 2009; Meli *et al*, 1988).

Anisotropy within the TG43 formalism is described by the quantity *F(r,θ)*. The introduction of the anisotropy of source distribution function *F(r,θ)*, is to account for the differences in dose rate as a function of angle from the symmetry axis due to the specific geometry of the encapsulation of the radioactive source. The 2D anisotropy is described by the TG43 model by:

$$F(r,\theta) = \frac{\dot{D}(r,\theta)G(r,\theta_o)}{\dot{D}(r,\theta_o)G(r,\theta)} \qquad (2.10)$$

The variation of dose rate about the source at every point around the source is expressed by equation (2.10) and this variation is mainly due to the effects of self-filtration, oblique filtration of primary photons through the encapsulating materials and scattered photons in the medium. The information on the dose rate in all directions provides a means to determine the anisotropy from the TG43 formalism, Monte Carlo modelling and the Sievert integral (Nath *et al* 1990)

If a substantial number of seeds are oriented haphazardly or the degree of dose anisotropy around single sources is restricted, the dose rate impact on tissue for each source can be estimated using the average radial dose rate. This is extended by adding

up the single anisotropic points due the seed sources (Nath *et al* 1990). Although the anisotropic function is a function of *r* and *θ*, the quantity *F(r,θ)* can be averaged over the *4π* geometry and *F(r,θ)* can be approximated using simple radial function $\phi_{an}(r)$, called the one dimensional (1D) anisotropy function which gives the same effect as the 2D anisotropy because of its averaging effects.

$$\dot{D}(r) = \frac{1}{4\pi}\int_{0}^{4\pi} D(r,\theta)d\Omega \qquad (2.11)$$

$d\Omega = 2\pi sin\theta d\theta$; for a cylindrically symmetric dose distribution (Ling *et al*, 1985).

Substituting equation (2.3) into (2.12) and rearranging, we obtain as shown in equation (2.13).

For scenarios where a 2D calculation cannot be used for cylindrical sources, the revised TG43 protocol which is called the TG43U1 recommends the use of

$$\dot{D}(r,\theta) = S_k \Lambda \frac{G(r,\theta_o)}{G(r_o,\theta_o)} g\, \phi_{an}(r) \qquad (2.12)$$

The quantity $\phi_{an}(r)$ describes the anisotropic factor which is a ratio of the dose rate at a distance ***r*** averaged with respect to a solid angle, to the dose rate on the transverse axis at the same distance (Nani *et* al, 2009) expressed as

$$\emptyset_{an}(r) = \frac{\int_0^{\pi} \dot{D}(r,\theta) sin\theta d\theta}{2\dot{D}(r,\theta_o)} \qquad (2.13)$$

For sources such as ^{192}Ir, ^{125}I and ^{103}Pb, $\phi(r)$ is less than one with values extending from 0.91 to 0.97.

Equation (2.13) displays more accuracy when dealing with cylindrical sources at distances less than 1 cm as compared to the rather oversimplified equation (2.1) with

the simple point source approximation. This is because for clinical line sources (thin cylinders) both ends of the source must have their orientation within the patient determined (Meli *et al*, 1988).

The universal recognition of the TG43 brachytherapy dose calculation model nonetheless has clinical limitations. Dose calculation formalisms based on the TG43 fail to account for dose distribution in finite tissues and heterogeneities in the patient, and the proper handling of the effects of shielding material in the calculation.

2.6 FAST FOURIER TRANSFORM

Fourier analysis of a periodic function involves extraction of the series of sine and cosine signals which when superimposed will reproduce the parent function. This analysis can be expressed as a Fourier series. The fast Fourier transform (FFT) is a mathematical method for transforming a function of time into a function of frequency (Kyeremeh, 2011). It is often considered as a translation from the time domain to the frequency domain and has proven to be very useful for analysis of time-dependent phenomena such as dose distribution.

Convolution which is a mathematical procedure that combines two functions in such a way to produce a third function. One of the input functions is the convolution kernel, or spread function (the energy deposition kernel in this case), and the two input functions are said to be convolved (Papanikolaou, 2004). Convolving two functions could be represented mathematically as:

$$h(x) = f(x)g(x) \qquad (2.14)$$

But

$$f(x)g(x) = \int f(\tau)g(x-\tau)d\tau = \int g(\tau)f(x-\tau)d\tau \qquad (2.15)$$

Where *f(x)g(x)* denotes convolution of the two functions *f* and *g*.

Convolution procedure at a given point *x* is calculated through correctly placing each element of the kernel *g(x)* and centring it at that point. The resultant elements of the primary functions (TERMA at *x*, and the kernel element at the same point) are then multiplied.

The goal of dose calculations is to find the reaction (TERMA) to a deposition of dose (KERMA – Kinetic Energy Released per unit Mass) in the tissue. The distribution of dose in 3D in the tissue is estimated by superimposing the point values of the absorbed dose from the knowledge of TERMA with reference to the dose deposition kernel. The dose distribution from the incident photon interaction point is illustrated by the kernel through the volume of the TERMA (Daskalov, 1998). Although the patient's main source of dose emanates from photons, the dose impact from beta particles is substantial to the dose close to the superficial part of the volume of the TERMA and this is usually justified for in the algorithm by modelling a photon-only dose and comparing it to the dose that has already been measured at shallow depths (Miften, 1999).

The method computes doses in a 3D configuration and fundamentally takes care of the influence of tissue heterogeneities on both incident and scattered photons (Papanikolaou, 2004). Apart from the corrections made for distribution of measured dose, the convolution calculates the distribution of dose from fundamental principles. The calculation is a four staged model which are:

1. Modelling the incident energy fluence as it exits the source (accelerator),
2. Projection of the energy fluence through the density representation of a patient to compute a TERMA volume,
3. Three-dimensional superposition of an energy deposition kernel and
4. Electron contamination model. (Papanikolaou, 2004)

The fast Fourier convolution technique follows from two functions *f(t)* and *g(t)* with their respective Fourier transforms as *F[f] and F[g]*. The convolution theorem states that, the Fourier transform of the convolution is the complex product of the individual Fourier transforms.

Thus

$$F[f * g] = F[f] \,.\, F[g] \qquad (2.16)$$

Hence convolving the two functions *f(t)* and *g(t)*, the result is given by:

$$f(t) * g(t) = \int_{-\infty}^{+\infty} f(\tau) g(t-\tau) d\tau \qquad (2.17)$$

The dose distribution at the point ***x*** by the conventional model is expressed as

$$D(x) = \int_{-\infty}^{+\infty} g(x') f(x-x') dx' \qquad (2.18)$$

Where,

$$g(x') = \sum_{i=1}^{N_s} S_i \delta(x-x') \qquad (2.19)$$

Equation (2.19) defines the geometric arrangements of the seeds and the corresponding strengths spatially described by the Dirac function $\delta(x)$. Equation (2.18) defines a convolution operation on the kernel *f(x)* with the a function *g(x)*. A solution to the equation (2.18) could be expressed in the form of an inverse Fourier transform (IFT), shown by equation 2.20:

$$D(x) = F^{-1}\left[\frac{1}{N}.F[g(x)].F[f(x)]\right] \qquad (2.20)$$

F^{-1} denotes the IFT and *N* is the sampling size. The extension of equation (2.20) in 3D gives the three dimensional dose distributions as (Kemmerer *et al*, 2000)

$$D(x) = F^{-1}\left[\frac{1}{N_x N_y N_z}.F[g(x,y,z)].F[f(x,y,z)]\right] \qquad (2.21)$$

2.6.1 Implementation of FFT Convolution

The discrete convolution of two discrete functions f_i *and* g_i with period *N*, defined by their samples $i = 0,1, \ldots \ldots N-1$, is given by

$$(f * g) = \sum_{k=-\frac{N}{2}+1}^{N/2} f_{i-k}g_k = \sum_{k=-\frac{N}{2}+1}^{N/2} g_{i-k}f_k \qquad (2.22)$$

The discrete nature of the convolution is based on the assumption that the two functions are periodic and of equal length. Their periodic nature leads to a wraparound effect which is prevented through the extension of the functions with zero padding. Since the FFT requires only positive indices, the putting into effect of equation (2.22) demands a shift of the function, and this is obtained by a wraparound ordering of one of the functions as shown in fig. 2.4.a. for three sources in a one

dimensional representation. The fig. 2.4.c. illustrates the kernel in a wraparound order necessary for FFT. The IFT of the function *g(x)* and the kernel *f(x)* is shown in fig. 2.4.g

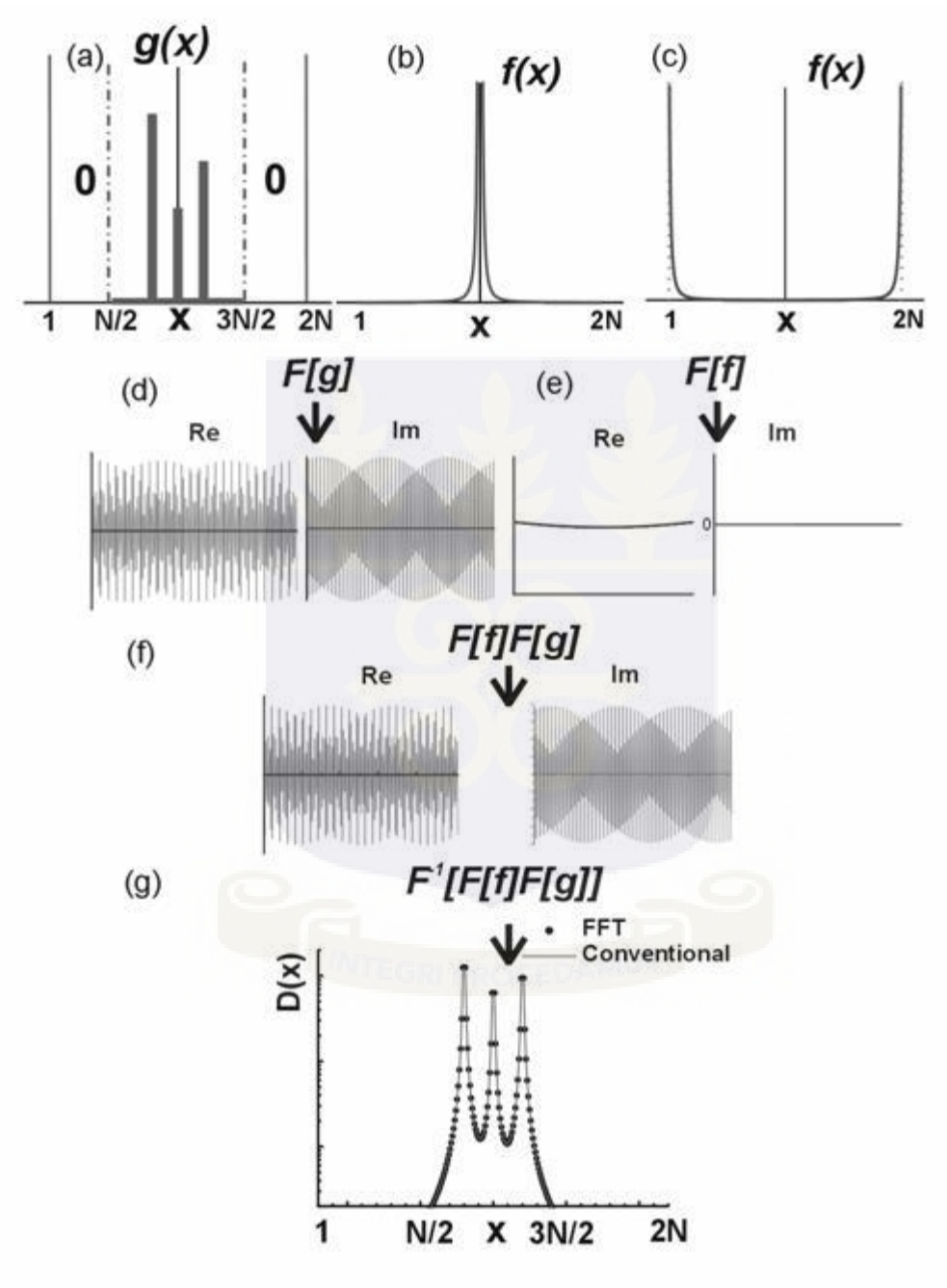

Figure 2.4: Schematic diagram illustrating the FFT convolution method for calculating the dose distribution for one dimensional case of three sources with different lengths

2.7 MONTE CARLO (MC) BASED DOSIMETRY

MC based dosimetry has been generally recognised as one very useful tool in curietherapy forming one of the dosimetric requirements for regular clinical use of modern low energy photon interstitial radiation sources (Williamson *et al* 1998; Weaver, 1998).

The MC procedure operates by performing a statistical simulation of every process related to photon transport and emission through the use of arbitrary numbers and suitable probability distribution functions. Its key feature is its probabilistic feature, implying that in contrast to some analytical procedures, each evaluation of a problem will, generally, yield varying results. The accuracy of the outputs is dependent, among other factors, on the number of statistical simulation processes. This makes MC calculations more rigorous and time-consuming than other analytical methods but the accessibility of computational resources and the major improvement in computer processor speed (although it requires a lot of resources) in the 21st century has greatly decreased calculation times. Nonetheless, MC simulation is still too CPU intensive to support commercial TPS. MC dosimetry has been carried out on sources such as ^{103}Pd and ^{125}I (low energy), ^{241}Am and ^{169}Yb (medium energy), and ^{192}Ir and ^{137}Cs nuclides (higher energy), but excludes rarely used ^{60}Co, and lots of discussions have been made for energies ranging from 20 to 700 keV such that electronic equilibrium may be safely assumed. This is to ensure that collision kerma is used to estimate absorbed dose and secondary electron tracking is omitted. Electronic non-equilibrium or imbalance occurs only at points in close proximity, such as those less than 1 mm, to high energy ^{192}Ir sources. However, dose rate improvement effect due to the emission of beta particles by ^{192}Ir has been observed in this distance range (Wang *et al*, 2000; Karaiskos *et al*, 2001; Baltas *et al*, 2001)

The foundation of any MC simulation code is a random number generator. It is important that this source of random numbers (R_N) results in an even distribution within the unitary interval [0, 1], and this means that all numbers that fall within this interval has equal probability.

In brachytherapy, MC based dose calculation in a given medium is a three-step procedure.

1. The energy fluence of photons emitted by the active source core must be simulated.
2. These photons must be transported through the source core and source encapsulation materials.
3. Photons must be transported in the medium near the source in order to evaluate the dose delivered in predefined volume elements: i.e., scoring voxels.

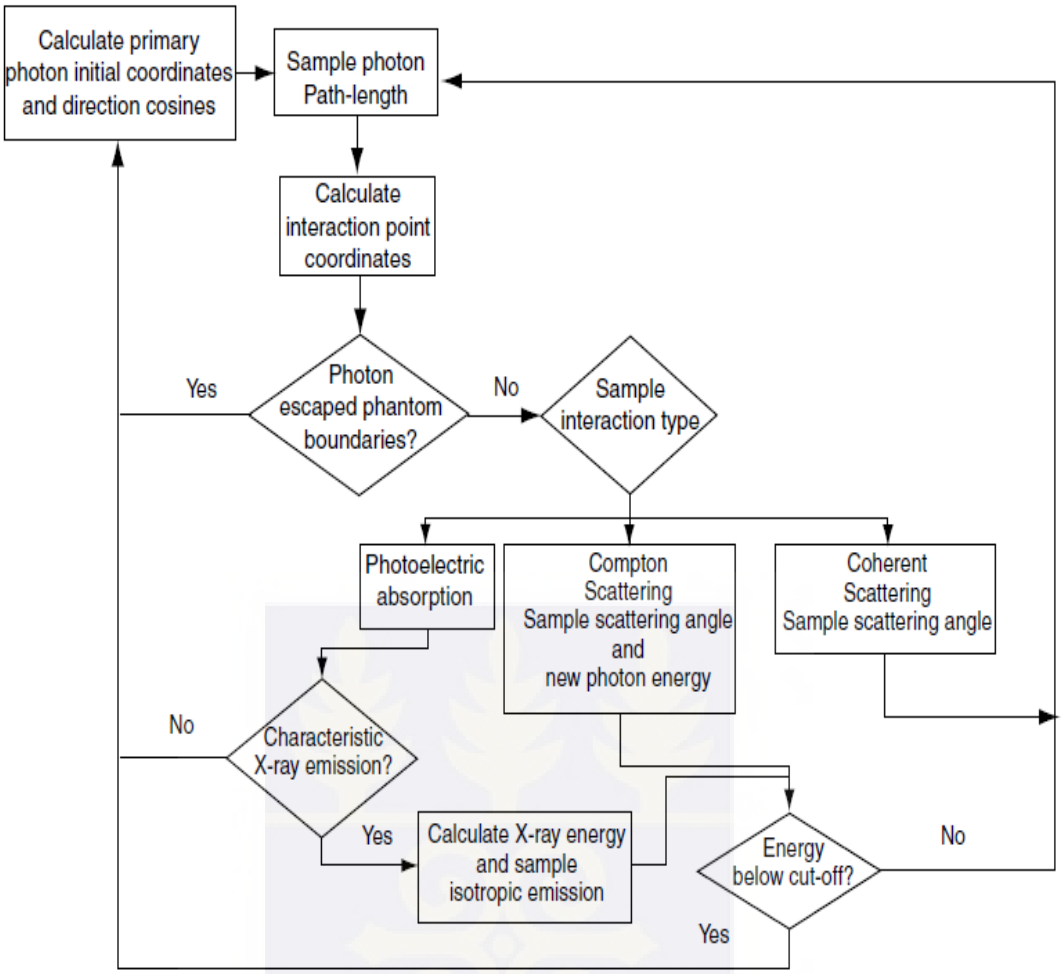

Figure 2.5: A pictorial representation of MC method of sampling primary and scattered radiation photons emitted by a radioactive source.

MC results from the above process could be analysed through comparison with non-stochastic quantities applicable to the simulation (Baltas *et al*, 2007).

2.8 SIEVERT INTEGRAL

The Sievert Integral was first introduced and named after its founder, Professor Rolf Maximilian Sievert; a Swedish professor of medical physics in 1921 and it has a general form (Sievert, 1921):

$$F(r,\theta) = \int_0^{\theta} e^{-x\sec\theta} d\theta \qquad (2.23)$$

It is a unique function usually encountered radiation transport related calculations. (Sievert Integral, http://en.wikipedia.org/wiki/Sievert_integral.html, 18th March, 2017). Since the introduction of the integral almost about ten decades ago, different models of the Sievert integral have been developed for the calculation of dose distribution in order to obtain much more accurate results. The most popular of all models is that used by Williamson *et al*, 1996, and it has been cited in other published works. Karaiskos *et al*, 2000, also implemented a different model, shown in equation 2.24, of the integral which was used by Pantelis *et al* in 2002.

$$\frac{\dot{D}(r,\theta)}{S_K} = \frac{1}{N}\left(\frac{\overline{\mu_{en}}}{\rho}\right)_{air}^{water} \sum_{i=1}^{N} \left\{ \frac{\left[\frac{e^{(-\mu_s \cdot s_i - \mu_f \cdot f_i - \mu_w s_i)}}{F(r_c)} + e^{(-\mu_w \cdot r)} \cdot SPR(r) \cdot C(r,\theta)\right]}{r_i^2} \right\} \quad (2.24)$$

$\dot{D}(r,\theta)$ = Dose rate

S_K = Source air kerma strength

N = number of small segments in which active source core is divided into

$\left(\frac{\overline{\mu_{en}}}{\rho}\right)_{air}^{water}$ = water-to-air ratio of mass-energy absorption coefficient

μ_s = linear attenuation coefficient of source

μ_f = linear attenuation coefficient of filter

μ_w = linear attenuation coefficient of water (medium of measurement)

$SPR(r)$ = Scatter-to-primary ratio of dose in water

$C(r,\theta)$ = Empiric correction describing the deviation of scatter radiation from isotropy

$F(r_c)$ = Normalization factor correcting that corrects for capsule filtration and is given by:

$$F(r_c) = \frac{1}{N}\sum_{i=1}^{N}\left[\frac{\left[e^{(-\mu_s \cdot s'_i - \mu_f \cdot f'_i)}\right]}{r'^2_i}\right] \qquad (2.25)$$

Various corrections are employed in implementing the Sievert integral for the calculation of dose to attain a targeted result

CHAPTER THREE

METHODOLOGY

3.1 SIEVERT INTEGRAL TECHNIQUE

The Sievert integral, equation (3.1), introduced in 1921 by Professor Sievert, is a method that can be used to calculate the exposure rate around a linear brachytherapy source. The method is implemented by dividing the line source into small elementary sources and putting into consideration inverse square law (ISL) and filtration corrections to each of these sources (Khan 2010)

$$F(r,\theta) = \int_0^{\theta} e^{-x\sec\theta} d\theta \qquad (3.1)$$

For a source with the following parameters:

L = active length

t = filtration

A = activity

Γ = exposure rate constant

μ'= effective attenuation coefficient for the filter

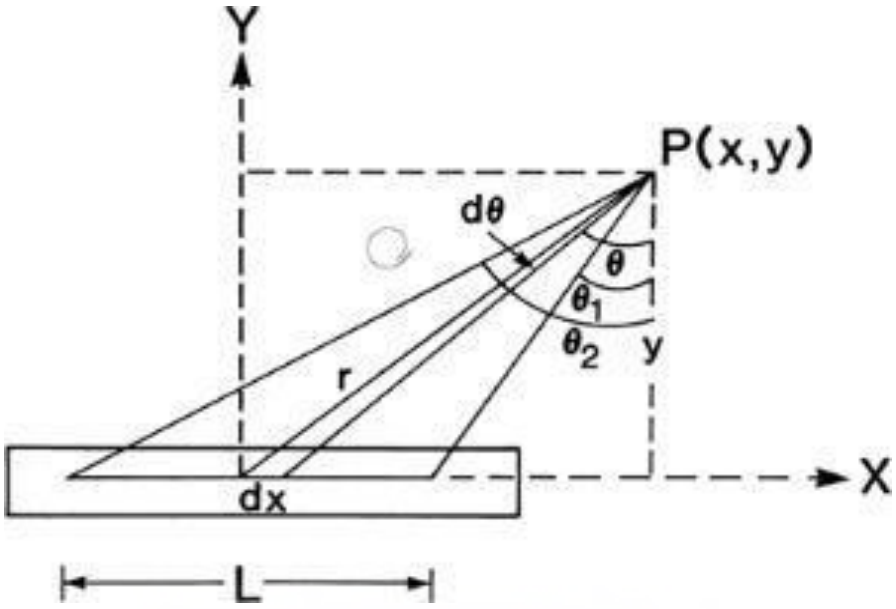

Figure 3. 1: Diagram displaying the geometric relations used in the evaluation of exposure at point P, from an elementary source. (Khan, 2007)

The exposure rate *dI* at a point *P(x,y)* contributed by the source element of length *dx*, as shown in fig 3.1 is given by:

$$dI(x,y) = \frac{A}{L} \cdot \Gamma \cdot dx \cdot \frac{1}{r^2} \cdot e^{-\mu' \cdot t \cdot \sec\theta} \qquad (3.2)$$

Making substitution with the following equations (3.3), (3.4) and (3.5):

$$r = \mathrm{y} \sec\theta \qquad (3.3)$$

$$x = \mathrm{y} \tan\theta \qquad (3.4)$$

$$dx = \mathrm{y} \sec^2\theta \, d\theta \qquad (3.5)$$

and integrating equation (3.2), the exposure rate *I(x,y)* obtained for the whole source:

$$I(x,y) = \frac{A\Gamma}{Ly} \int_{\theta_1}^{\theta_2} e^{-\mu' \cdot t \cdot \sec\theta} d\theta \qquad (3.6)$$

Equation (3.6) takes after (3.1) which is the general form of the Sievert integral. The above Sievert integral may be evaluated by numerical methods but this would not be done in the case of this research.

For a source with intensity specified in terms of exposure rate $\dot{X}_s$ at a specified distance, ***s***, far from the source (i.e. $s \gg L$), then the Sievert integral can be written as:

$$I(x,y) = \frac{\dot{X}_s \cdot s^2}{Ly} \cdot e^{\mu' t} \int_{\theta_1}^{\theta_2} e^{-\mu' \cdot t \cdot \sec\theta} d\theta \qquad (3.7)$$

The source strength used for this research is specified in air kerma strength, hence the Sievert integral model that will be implemented is:

$$I(x,y) = \frac{S_K}{Ly\left(\frac{\bar{W}}{e}\right)} \cdot e^{\mu' t} \int_{\theta_1}^{\theta_2} e^{-\mu' \cdot t \cdot \sec\theta} d\theta \qquad (3.8)$$

3.2 DOSE CALCULATION

Equation 3.8 calculates the exposure rate from the source, hence the need for conversion to dose. This was done by multiplying the emergent exposure rate expression by a quantity, f_{med} or simply the *f-factor* which is sometimes called the roentgen-to-rad conversion factor. This factor is a constant dependent on the medium in which measurement is done (in this case, water) and the photon energy from the radioactive source. Tables containing the values of the f_{med} were referred to and the value for a ^{60}Co photon energy, 1.25 MeV, in water is 37.6 Gy.kg/C. Aside the value of the constant being available in tables, the f_{med} can be calculated using equation 3.9 below.

$$f_{med} = 0.876 \frac{(\bar{\mu}_{en}/\rho)_{medium}}{(\bar{\mu}_{en}/\rho)_{air}} \qquad (3.9)$$

For a dimensional balance, the average work done per unit charge, $\frac{\overline{W}}{e}$, was converted from

0.876 cGy/R to cGykg/C using the factor:

$$1R = 2.58 \times 10^{-4} C/kg \qquad (3.10)$$

After the introduction of the *f-factor*, the resulting quantity is the dose rate. The dose is then calculated by multiplying the dose rate by the source dwell time (t_{dwell}) or treatment time which will be produced by HDR 3.0 Plus treatment planning system.

The equation (3.8) then becomes modified into equation (3.11) for calculation of the dose around the new BEBIG ^{60}Co source.

$$D = \frac{f_{med} \cdot S_K \cdot t_{dwell}}{L \cdot x \cdot \left(\frac{\overline{W}}{e}\right)} \cdot e^{\mu' t} \int_{\theta_1}^{\theta_2} e^{-\mu' \cdot t \cdot \sec\theta} d\theta \qquad (3.11)$$

The variable *x* in equation 3.11 has been used to replace *y* in equation 3.8 because the CP (point of measurement), unlike what is illustrated in figure 3.2 is on the *x* or horizontal axis while the source is on the *y* or vertical axis.

3.3 MATLAB

MATLAB is a powerful programming tool for handling the calculations (simple and complex) involved in scientific and engineering problems. The name MATLAB is an acronym which stands for MATrix LABoratory, because the system was designed to make computations of matrices particularly easy (Hahn and Valentine, 2007).

This programming tool distinguishes itself from others such as C++ and Java in the sense that it is user friendly and very interactive. This implies that you input some commands at the unique MATLAB prompt, known as the command window, and

obtain results immediately. The tool solves problems ranging from simple ones such as, finding a square root, or complex ones, like deriving the solution to a set of differential equations or solving an integral such as the Sievert integral. For some quite technical problems it would be required to enter just a few commands, and the answers are produced. (Hahn and Valentine, 2007)

The derived equations and the values for each parameter were used to write a MATLAB program and the calculations of the dose for each control point were obtained. One of such is displayed in figure 3.2.

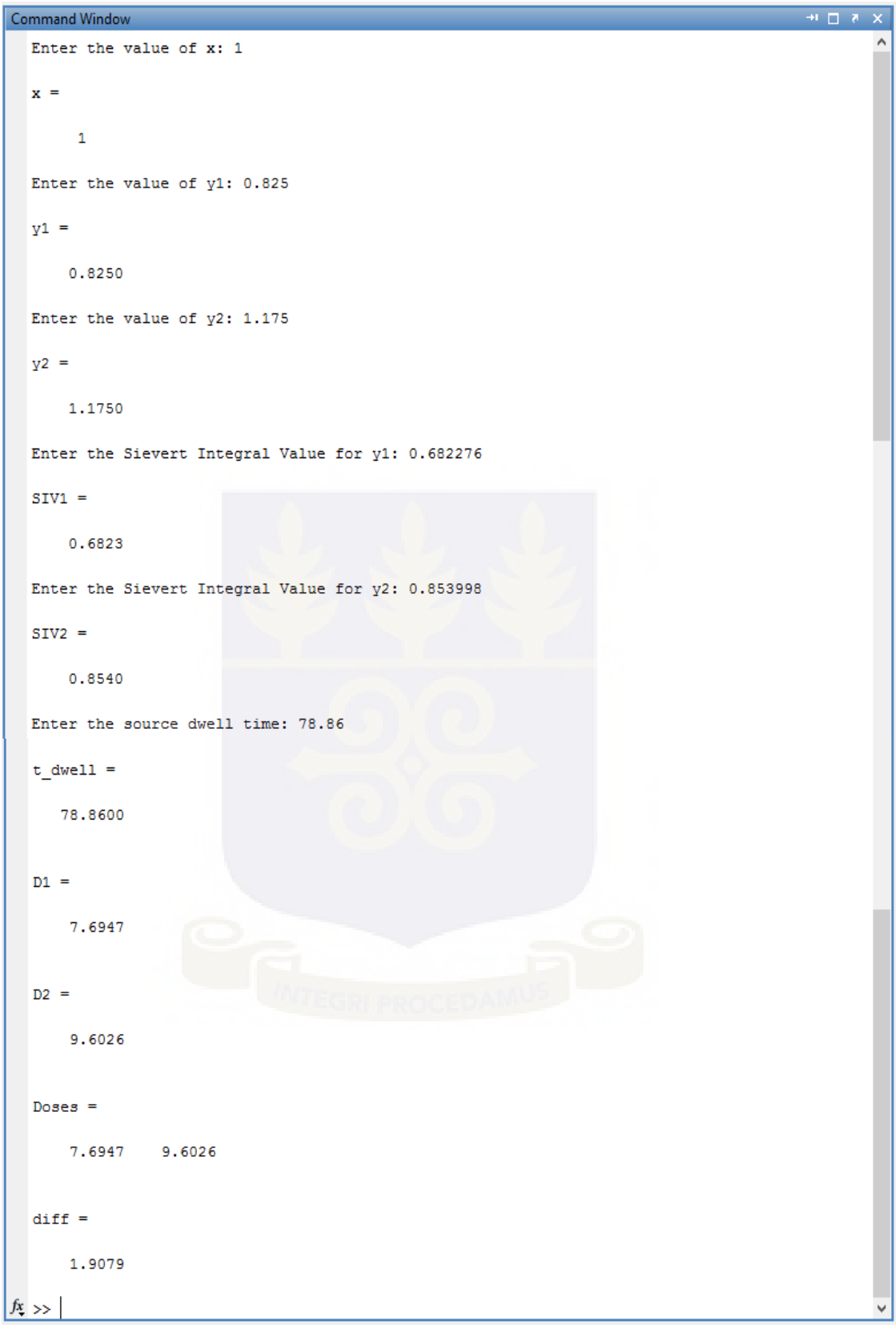

Figure 3. 2: Display of the dose calculation in the command window of MATLAB

3.4 IMPLEMENTATION OF THE SIEVERT INTEGRAL

An analytical solution of the Sievert integral does not exist; hence it will require either a numerical procedure or the use of a Sievert integral table of values such as that in appendix L.

The Sievert integral in equation (3.11) has to be modified due to the difference in the definite interval between that in 3.11 [θ_1, θ_2] and that used in the Sievert integral table [0, θ] which is identical to equation 3.1 and represented in equations 3.12 and 3.13

$$D1 = \frac{f_{med} \cdot S_K \cdot t_{dwell}}{L \cdot x \cdot \left(\frac{\bar{W}}{e}\right)} \cdot e^{\mu' t} \int_0^{\theta_1} e^{-\mu' \cdot t \cdot \sec\theta} d\theta \qquad (3.12)$$

$$D2 = \frac{f_{med} \cdot S_K \cdot t_{dwell}}{L \cdot x \cdot \left(\frac{\bar{W}}{e}\right)} \cdot e^{\mu' t} \int_0^{\theta_2} e^{-\mu' \cdot t \cdot \sec\theta} d\theta \qquad (3.13)$$

The variation in the angles under consideration in this research and those used in obtaining the integral values in the table, and the corresponding ***x***-values were obtained through extrapolation and interpolation calculations. The ***x*** used in equation 3.11 differs from that in equation 3.1. In comparison to that in 3.1, the product of the effective attenuation coefficient, μ', calculated using an equation (3.14) given by Williamson *et al* , and the wall thickness, *t*, which is 0.05 cm, yielded the value of *x*.

$$\mu'(d) = -\left(\frac{1}{d}\right) ln\left[\frac{\sum_i p_i E_i \left(\frac{\mu_{en}}{\rho}\right)_i^{air} e^{-\mu_{en}^i \cdot d}}{\sum_i p_i E_i \left(\frac{\mu_{en}}{\rho}\right)_i^{air}}\right] \qquad (3.14)$$

Where p_i= denotes the number of photons with energy E_i emitted per disintegration

$\left(\frac{\mu_{en}}{\rho}\right)_i^{air}$ = mass energy absorption coefficient in air for photon of energy E_i

d = filter thickness

E_i = photon energy

The value of the attenuation μ_{en} substituted into equation 3.14 to calculate for the effective attenuation co-efficient of the filter material for the source energy being considered, is the fitted value for the attenuation of the filter, μ_f = 0.25cm^{-1}. This was to ensure accuracy in calculated values and minimise the deviations between the Sievert model and any other model it is compared to which in this case is the TG43 (Nath *et al*, 1995). The other values for the attenuation are shown in table 3.1.

Table 3 1: Actual and fitted values of linear attenuation co-efficient for source and filtration materials μ_s and μ_f, respectively for the new BEBIG source.

(Bhola *et al*, 2012)

Linear attenuation co-efficient	$\mu_s(cm^{-1})$	$\mu_f(cm^{-1})$
Actual value	0.47	0.43
Fitted values	0.25	0.25

The Sievert integral value for each angle, θ_1, and θ_2, were obtained individually and the expression for their doses and a correction factor, calculated using the Meisbeger polynomial (equation 3.15), were multiplied. The difference in the doses obtained for each angle yielded the dose at the specified control point. All calculations were done by a MATLAB program as displayed in figure 3.

$$M_{poly} = A + Br + Cr^2 + Dr^3 \qquad (3.15)$$

$$r = \sqrt{x^2 + y^2} \qquad (3.16)$$

Where M_{poly} = Meisberger polynomial/function

r = distance from the source to control point calculated using x and y values

A, B, C and D are constants or polynomial coefficients whose values are source dependent and for ^{60}Co:

$$A = 0.99423 \quad (3.17)$$

$$B = -0.005318 \quad (3.18)$$

$$C = -0.002610 \quad (3.19)$$

$$D = 0.0001327 \quad (3.20)$$

3.5 NEW BEBIG ^{60}Co SOURCE

The radioisotope used for this research is ^{60}Co and its details are given in table 3.2. ^{60}Co as a source is more economical for use in a brachytherapy treatment unit due to its longer half-life (5.26 years) in comparison with ^{192}Ir. It is a well-established and clinically proven isotope for all HDR brachytherapy treatments. Co-60 sources are available for SagiNova, MultiSource and GyneSource afterloaders and since their introduction, lots of tremendous successes have been achieved. It has shown to be a good choice for treating gynaecological, rectal, prostate, dermatological and other body sites.

Treatment with Co-60 guarantees lower dose to OAR as compared to Ir-192 and this is due to its higher average energy of 1.25 MeV, hence less scatter is produced in its photon interaction with tissues. The Eckert & Ziegler BEBIG Co-60 source is loaded with an activity of about 81.4GBq. The capsule design of the source fulfils the demanding regulatory and governmental standards of the EU and other nations. The capsule and source wire are connected by high quality laser welding method and

crafted to withstand 100,000 source transfers. This has been verified by stress tests in straight and curved applicators exceeding this figure to ensure safety and long-term precision. With a value of 100, 000 cycles in a period of five years, the brachytherapy unit of a clinic could have an estimate of up to seven patients a day receiving a ten channel interstitial treatment or twenty-four patients a day for the treatment with a three-channel applicator.

The new model of the BEBIG ^{60}Co HDR (model Co0.A86) brachytherapy source design has a small active core with a diameter of 0.5mm and a more rounded capsule tip as compared to the old BEBIG source design. Its central cylindrical active core length is 3.5mm which is made of metallic ^{60}Co. This active core is covered by a cylindrical stainless steel capsule with an external diameter of 1.0 mm (more details are given in figure3.3)

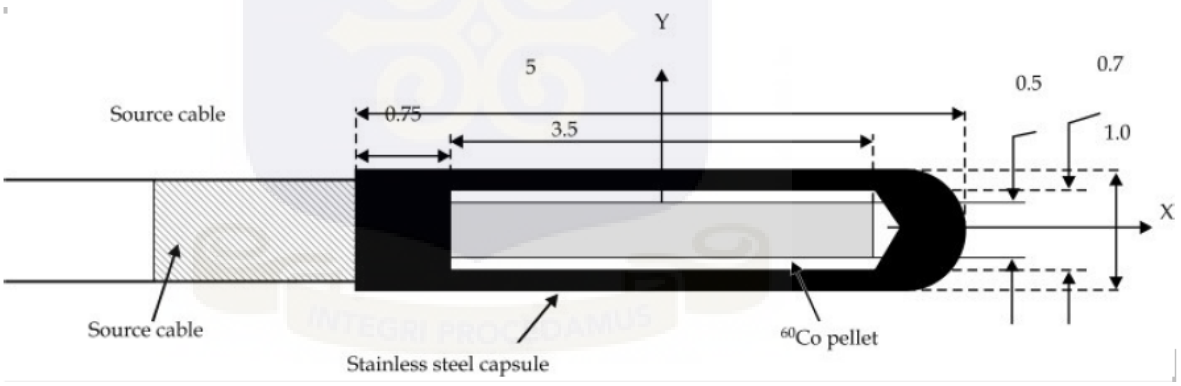

Figure 3. 3: Schematic diagram of the new BEBIG 60Co HDR brachytherapy source

Table 3 2: Details of the BEBIG Co-60 source including some initial parameters and their corresponding values by 18th March, 2017 which is the date of measurement.

Parameter	Value
Source Name	Multisource Co-60 HDR
Radionuclide	Co-60
Model Number	Co0.A86
Serial Number	BB-AC 547
Initial values [18th Jul, 2014]	
Air KERMA Strength	23210 cGy.cm^2/h
Activity in GigaBecquerel	78.85 GBq
Activity in Curie	2.05 Ci
Activity for planning [18th Mar, 2017]	
Air KERMA Strength	16343.6 cGy.cm^2/h
Activity in GigaBecquerel	53.41 GBq
Activity in Curie	1.4435 Ci

3.6 EQUIPMENT

The TPS used in the simulation of the sources is the HDRplus manufactured by BEBIG. It provides treatment comfort due to its user friendly interface (displayed in figure 3.4), it's fast flexible, precise and delivers an optimised treatment plan. The HDRplus supports all HDR applications, including intracavitary, interstitial and intraoperative treatments.

Its user interface features an ultramodern and easy-to-use structure with the many options to customise the layout and parameter settings which further allows the user to decide a personal planning approach. Another unique feature of the HDRplus is the complete applicator database which is used to select applicators and place them directly on an X-ray film or CT/MR images which eliminates the procedure of lengthy reconstruction of the applicator. The automated nature of the applicator reconstruction makes the HDRplus to identify implanted breast needles and visualise them in 3D for simplification of the treatment planning. Automatic image fusion feature of this treatment planning system enables its users to match CT and MR images without any user interference within a time frame of less than 30 seconds.

Figure 3. 4: Monitor displaying the interface of the HDRplus

The version of the HDRplus TPS used for the procedure is version 3.0.5. The software was launched from the desktop of the system and a patient profile with name "Sievert integral" was created. The universal applicator with a dimension of 12cm and name LLA1200-20 was selected and a (0,0) dose plane was defined on the orthogonal view. The origin was also defined, i.e. (0,0) point and the midpoint, 5.5 cm, of the source location in the applicator was placed on the (0,0) point.

CPs were generated with a spacing of 1 cm apart on the *x*-axis to the left and right of the

y-axis. A prescribed dose of 2 Gy was normalised to the *x* = 1 cm CP which is the first point from the origin. The TPS generated a dose distribution and the doses to the various CPs were recorded. The same procedure was repeated for the (0,1), (0,2), (0,-1) and (0,-2) cm points as clearly illustrated in figures 3.5a to 3.5e.

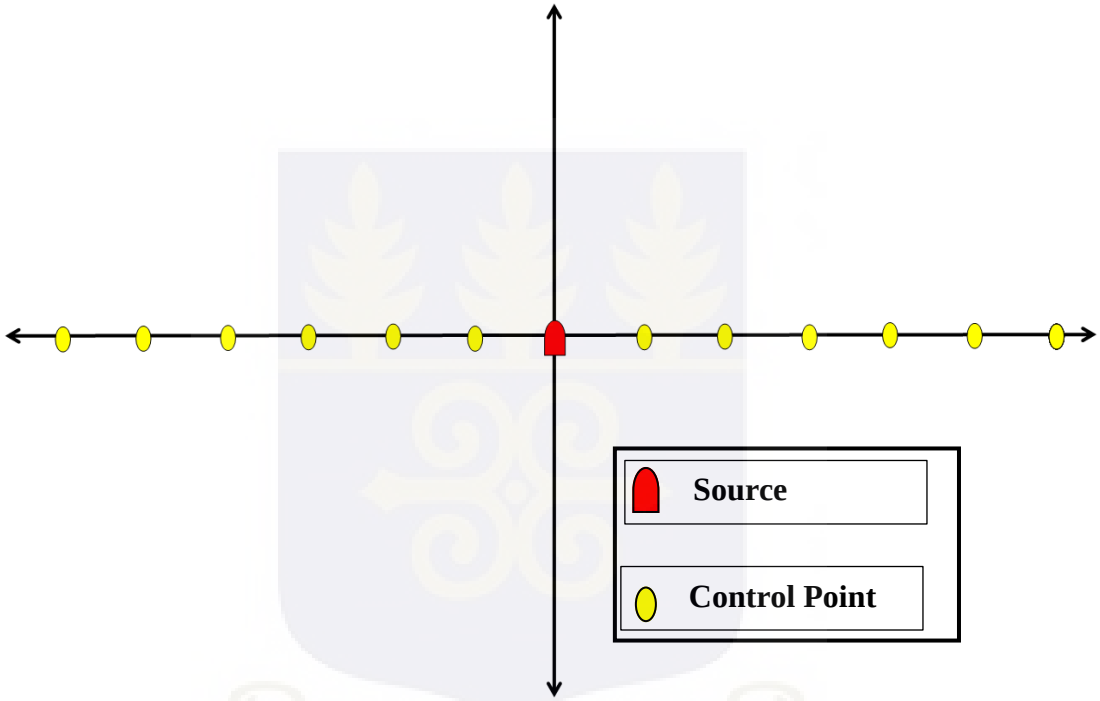

Figure 3.5 a: Source dwell position at y = 0 cm

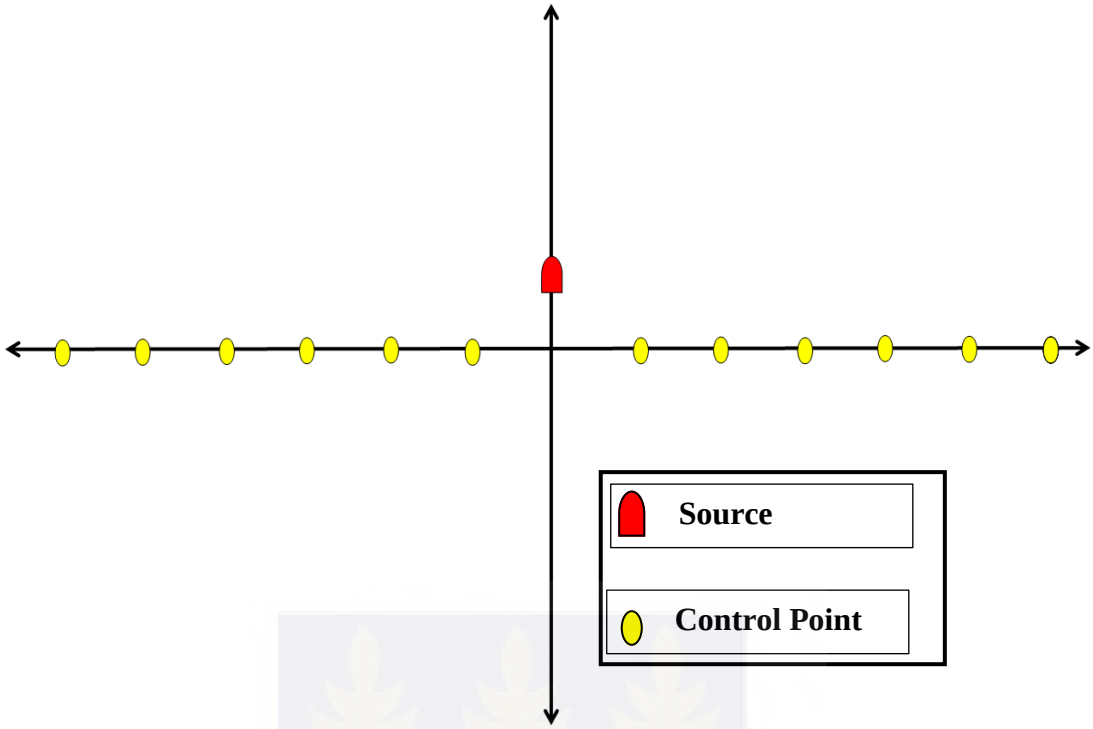

Figure 3.5 b: Source dwell position at y = 1 cm

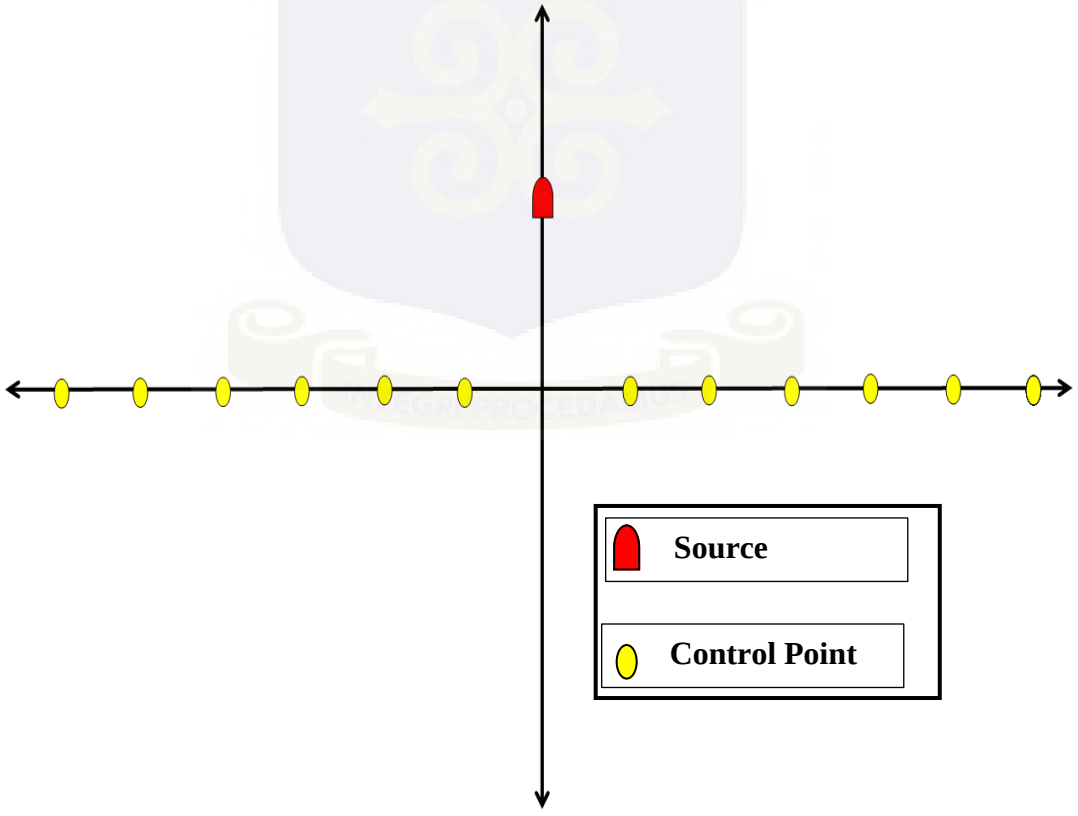

Figure 3.5 c: Source dwell position at y = 2 cm

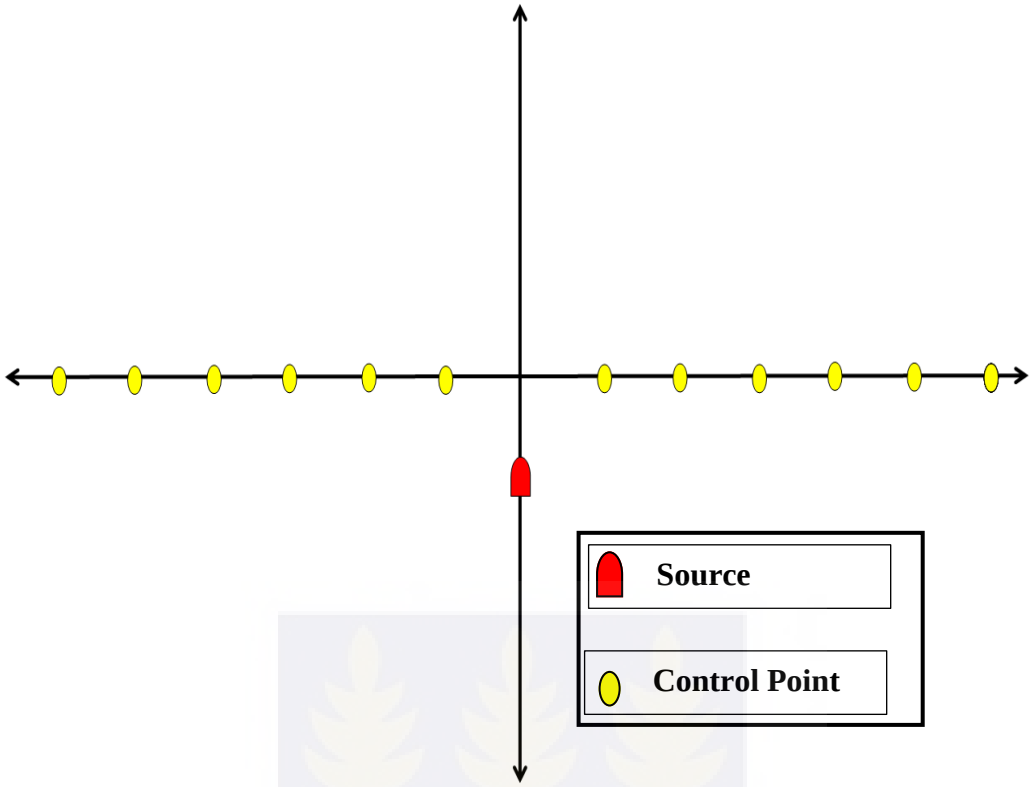

Figure 3.5 d: Source dwell position at y = -1 cm

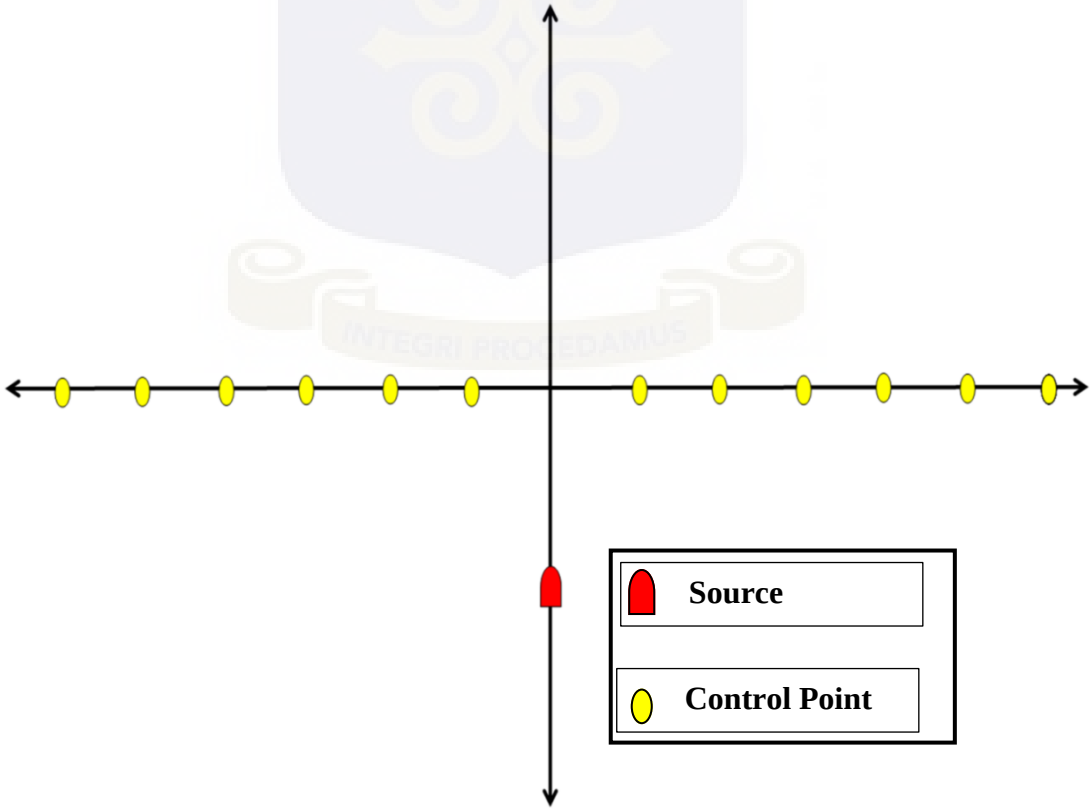

Figure 3.5 e: Source dwell position at y = -2 cm

3.7 AAPM TG 43 DOSE CALCULATION FORMALISM

The TG43 report (Nath *et al*, 1995, Rivard J *et al*, 2004) recommended the dose calculation algorithm for establishing the two-dimensional dose rate distribution in a water medium around cylindrically symmetric photon-emitting brachytherapy sources. The TG 43 formalism, which is well expatiated in chapter two, is a more advantageous method because it contains quantities or parameters measured solely in the medium. The data for a specific source can be compiled as a function of position and the effects of several physical factors on the value of the dose rate distribution are considered separately. (Kyeremeh, 2011)

3.8 COMPARISON OF SIEVERT INTEGRAL VALUES AND HDRplus RESULTS

The dose obtained from the two methods were analysed by producing a bar chart of dose against control point for each dwell position. In addition to the bar chart, two curves on the same plane for both methods, per dwell position were also plotted. These graphical representations were done for better understanding of the deviation of the outcomes of the two procedures.

Percentage deviations of the Sievert integral dose values from that of the HDRplus which was designed based on the TG 43 algorithm, were calculated using the relation

$$\%\ Deviation = \frac{\left|D_{SI} - D_{HDRplus}\right|}{D_{HDRplus}} \times 100\ \%$$

Where D_{SI} = Dose from Sievert integral

$\boldsymbol{D_{HDRplus}}$ = Dose from HDRplus

CHAPTER FOUR

RESULTS AND DISCUSSION

4.1 HDRplus Dose Computations

From the procedures spelt out in section 3.6, the acquired results for the individual control points are shown in the tables 4.1 to 4.5 and the corresponding isodose lines in figures 4.1 to 4.5.

Table 4 1: CP parameters for Source at y = 0 cm

Prescribed Dose (Gy)	2.00
Total Dwell Time (s)	40.25
Dwell Position (cm)	(0,0)
Total Reference Air Kerma (cGy.m^2)	0.01827
Minimum Dose (Gy)	0.05
Average Dose (Gy)	0.49
Maximum Dose (Gy)	2.00

Table 4 2: Dose Control Point Report for Source at y = 1 cm

Prescribed Dose (Gy)	2.00
Total Dwell Time (s)	78.68
Dwell Position (cm)	(0,1)
Total Reference Air Kerma (cGy.m^2)	0.03572
Minimum Dose (Gy)	0.1
Average Dose (Gy)	0.6
Maximum Dose (Gy)	2.00

Table 4 3: Dose Control Point Report for Source at y = 2 cm

Prescribed Dose (Gy)	2.00
Total Dwell Time (s)	202.72
Dwell Position (cm)	(0,2)
Total Reference Air Kerma (cGy.m^2)	0.09203
Minimum Dose (Gy)	0.23
Average Dose (Gy)	0.84
Maximum Dose (Gy)	2.00

Table 4 4: Dose Control Point Report for Source at y = -1 cm

Prescribed Dose (Gy)	2.00
Total Dwell Time (s)	81.81
Dwell Position (cm)	(0,-1)
Total Reference Air Kerma (cGy.m^2)	0.03714
Minimum Dose (Gy)	0.1
Average Dose (Gy)	0.61
Maximum Dose (Gy)	2.01

Table 4 5: Dose Control Point Report for Source at y = -2 cm

Prescribed Dose (Gy)	2.00
Total Dwell Time (s)	208.64
Dwell Position (cm)	(0,-2)
Total Reference Air Kerma (cGy.m^2)	0.09472
Minimum Dose (Gy)	0.24
Average Dose (Gy)	0.85
Maximum Dose (Gy)	2.01

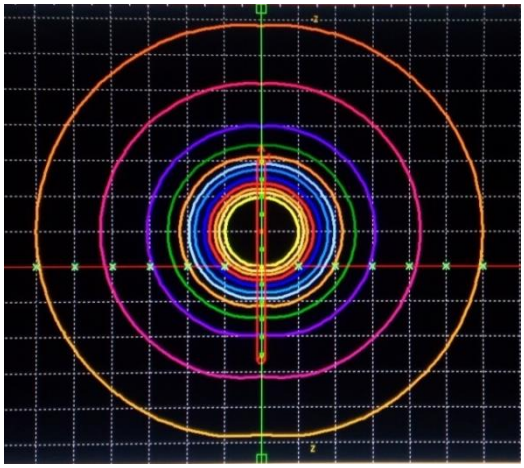

Figure 4. 1: Isodose lines for source at y = 1 cm

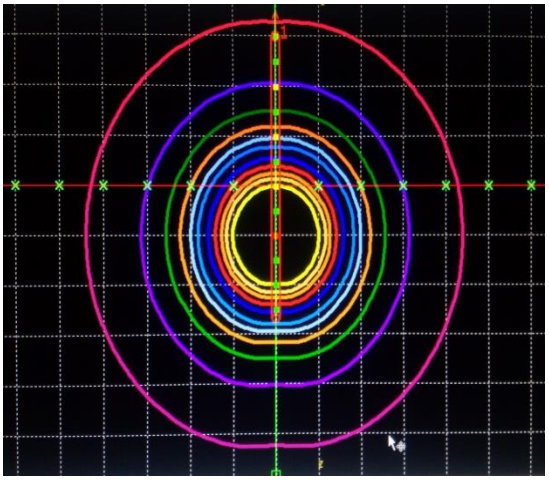

Figure 4. 2: Isodose lines for source at y = -1 cm

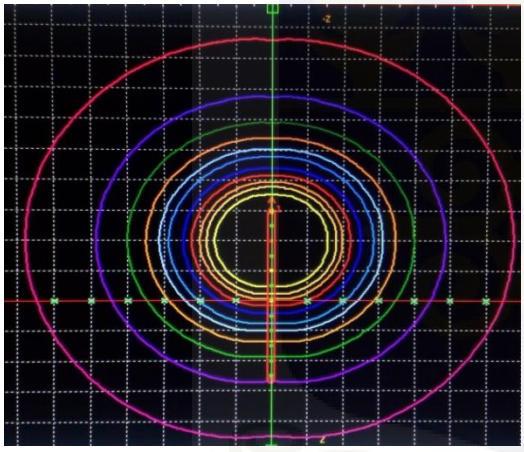

Figure 4. 3: Isodose lines for source at y = 2 cm

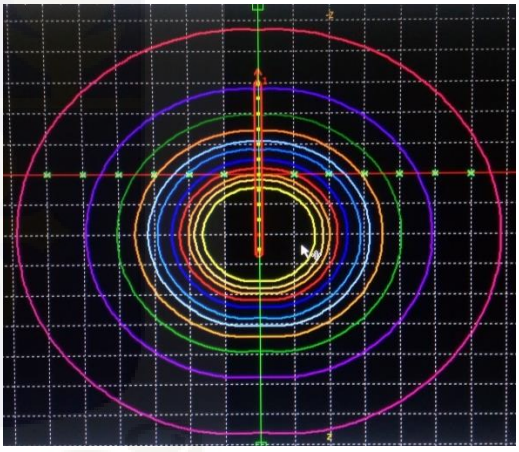

Figure 4. 4: Isodose lines for source at y = -2 cm

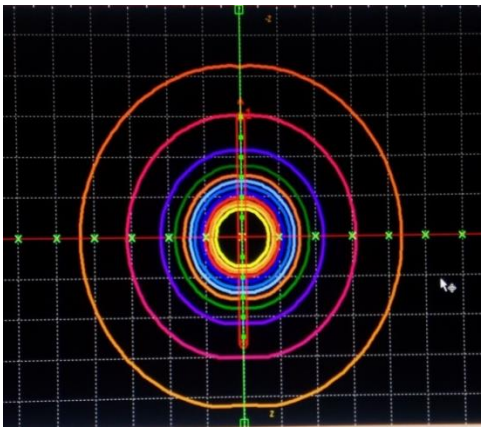

Figure 4. 5: Isodose lines for source at y=0 cm

4.2 SIEVERT INTEGRAL RESULTS

The computations from the Sievert integral yielded results recorded in tables for each control point. The dose outcome to control points equidistant and at equal subtended angles from the source, which were to the left and right of the source were equal. Therefore, x values represented in the following tables, for this section, are the absolute values of x.

The Sievert integral could not be used in calculating the dose delivered to the various control points when the source was positioned at the perpendicular bisector, i.e. at (0, 0), and this was because the angle or value of θ is equal to zero.

4.3 ANALYSIS OF RESULTS

The means of the doses recorded at each control with equal distance and oblique directions from the source were calculated to carry out comparison of the obtained dose values from both methods under consideration. Tables of values showing both sets of dose values for each source dwell positions and the corresponding deviations.

Table 4 6: Comparison of dose values for both methods for source at y = 1cm

Sievert_Dose(Gy)	HDR_Plus_Dose(Gy)	% Deviation
1.9036	1.9950	4.58
0.7603	0.7800	2.53
0.3752	0.3800	1.26
0.2170	0.2200	1.36
0.1386	0.1400	1.00
0.0953	0.1000	4.70

Table 4 7: Comparison of dose values for both methods for source at y = 2 cm

Sievert_Dose(Gy)	HDR_Plus_Dose(Gy)	% Deviation
1.7854	1.9950	10.51
1.1702	1.2400	5.63
0.7225	0.7500	3.67
0.4638	0.4800	3.38
0.3137	0.3200	1.97
0.2230	0.2300	3.04

Table 4 8: Comparison of dose values for both methods for source at y = -1 cm

Sievert_Dose(Gy)	HDR_Plus_Dose(Gy)	% Deviation
1.9793	2.0050	1.28
0.7905	0.7900	0.06
0.3901	0.3900	0.03
0.2256	0.2300	1.91
0.1442	0.1500	3.87
0.0990	0.1000	1.00

Table 4 9: Comparison of dose values for both methods for source at y = -2 cm

Sievert_Dose(Gy)	HDR_Plus_Dose(Gy)	% Deviation
1.8375	2.0050	8.35
1.2043	1.2500	3.66
0.7436	0.7600	2.16
0.4774	0.4900	2.57
0.3229	0.3300	2.15
0.2295	0.2400	4.37

Subsequently, bar charts and curves were plotted to illustrate how clearly the two methods'dose outcome deviate from each other with respect to the control points.

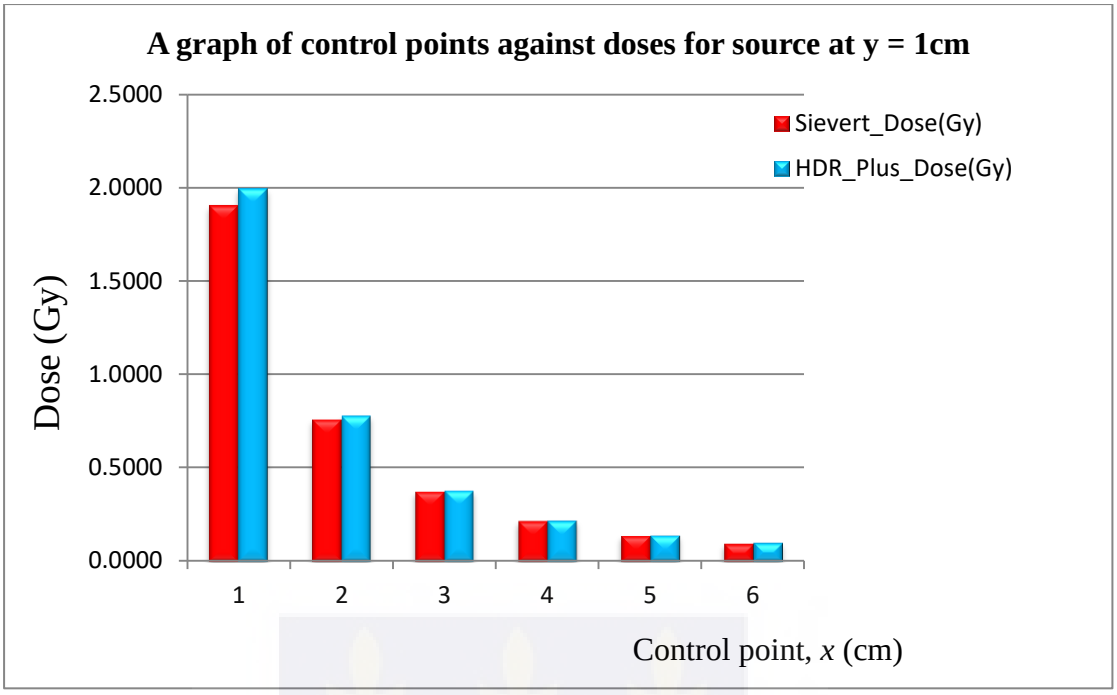

Figure 4. 6: Bar charts comparing dose outputs for source at y = 1cm

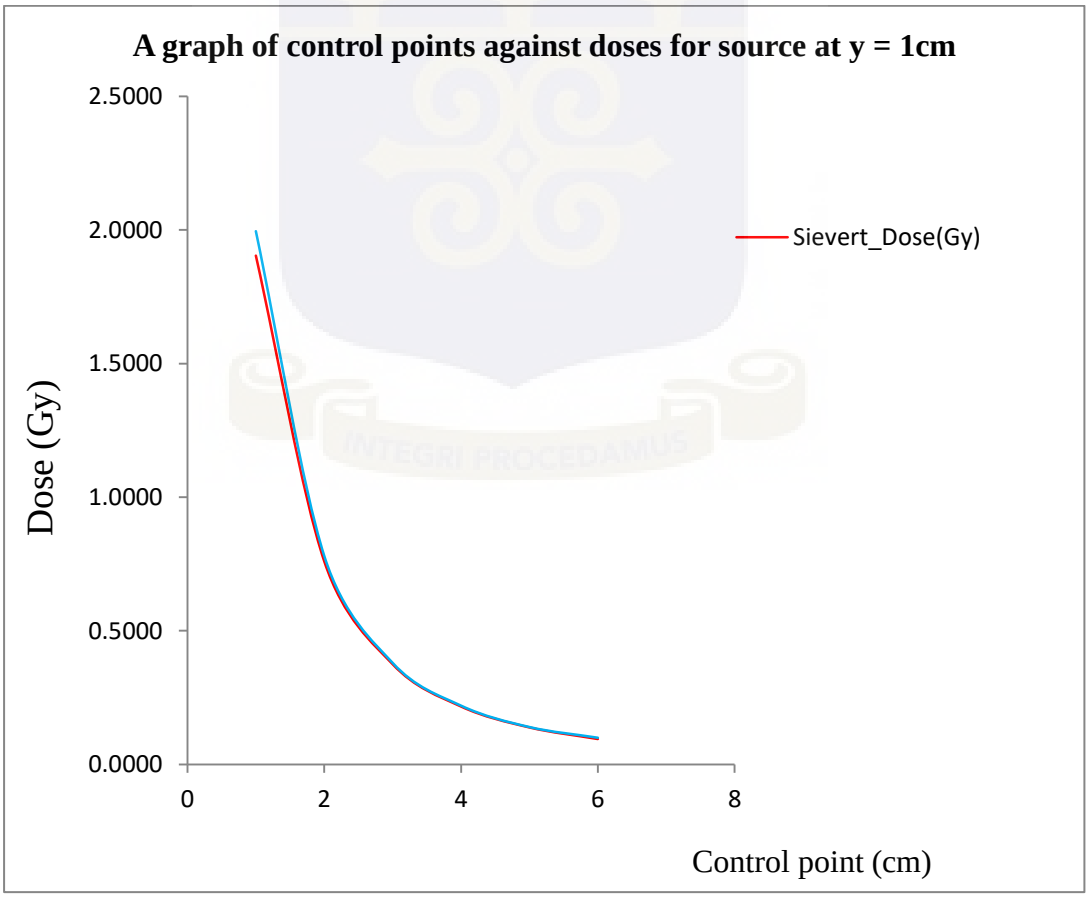

Figure 4. 7: Curves to compare dose outputs for source at y = 1cm

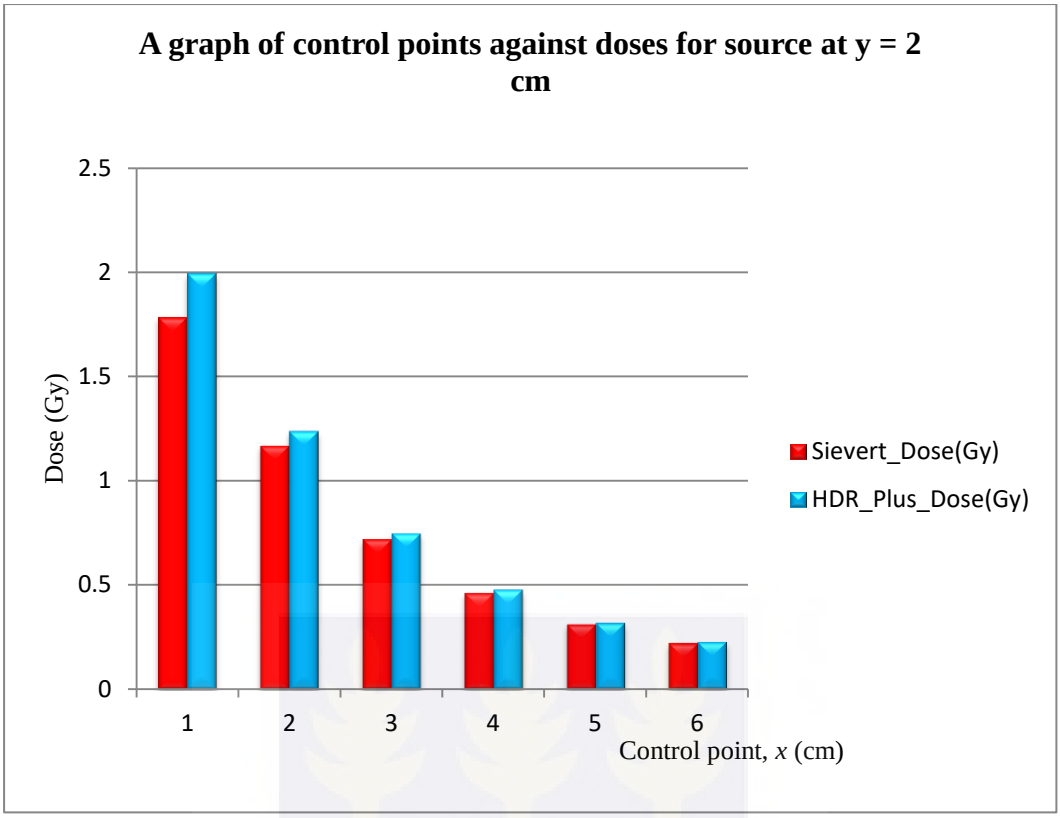

Figure 4. 8: Bar charts comparing dose outputs for source at y = 2cm

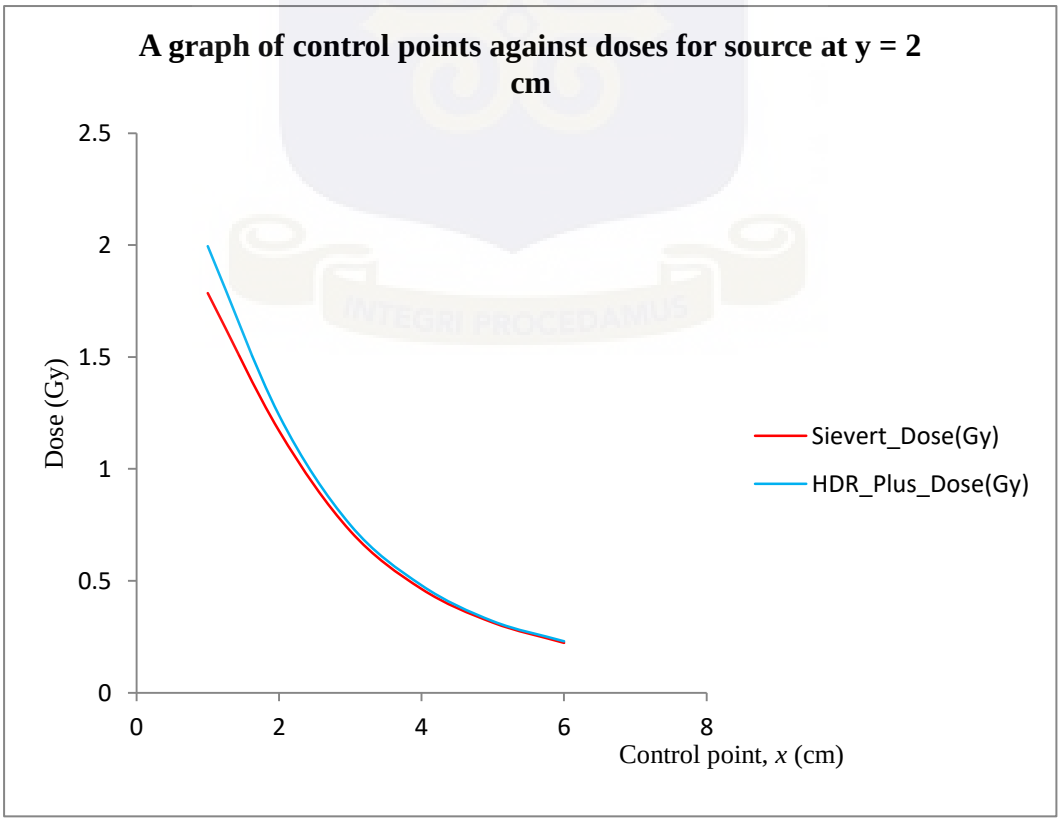

Figure 4. 9: Curves to compare dose outputs for source at y = 2

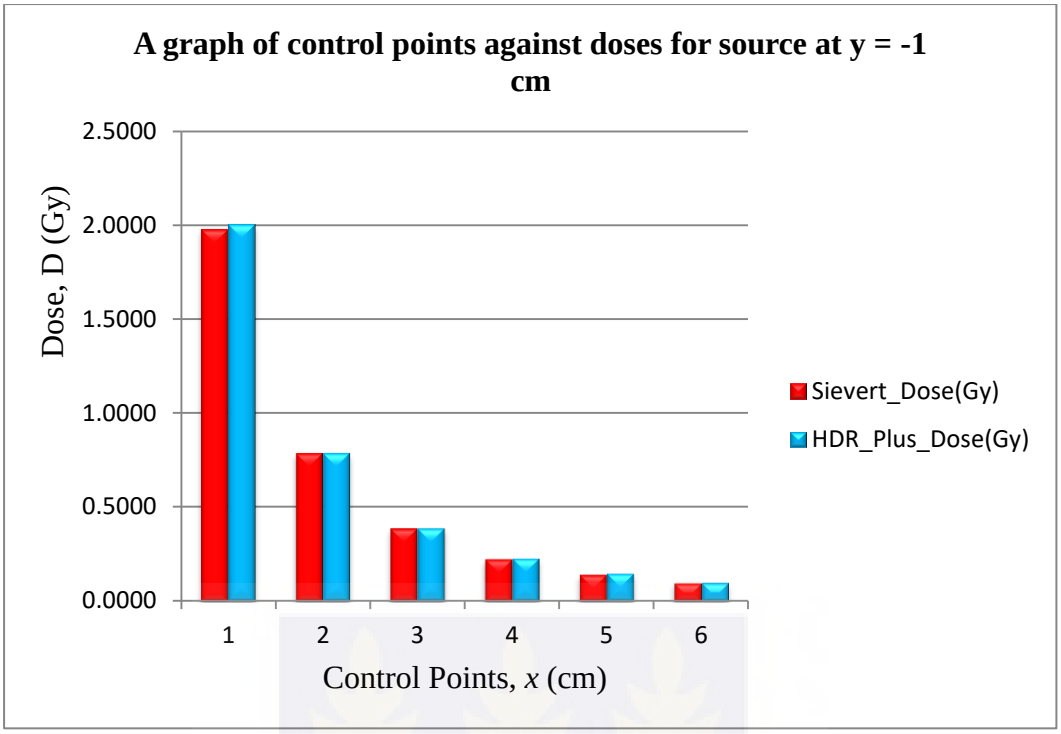

Figure 4. 10: Bar charts comparing dose outputs for source at y =- 1cm

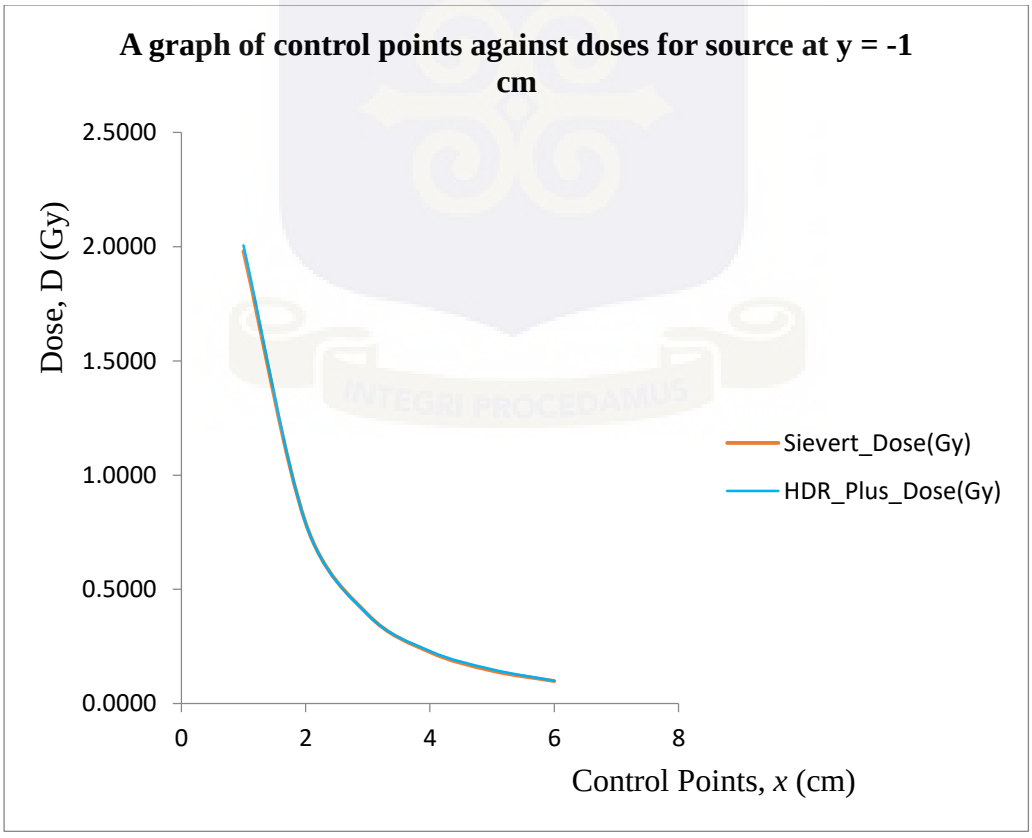

Figure 4. 11: Curves to compare ose outputs for source at y = -1cm

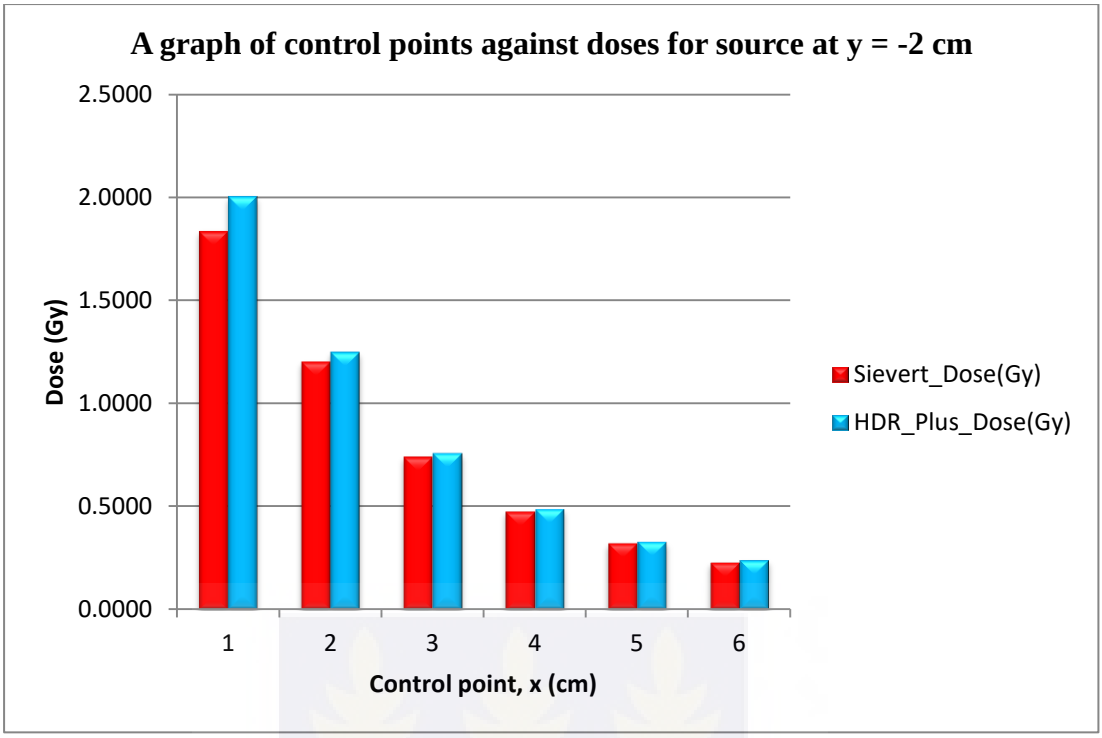

Figure 4. 12: Bar Charts for comparing dose outputs at y = -2cm

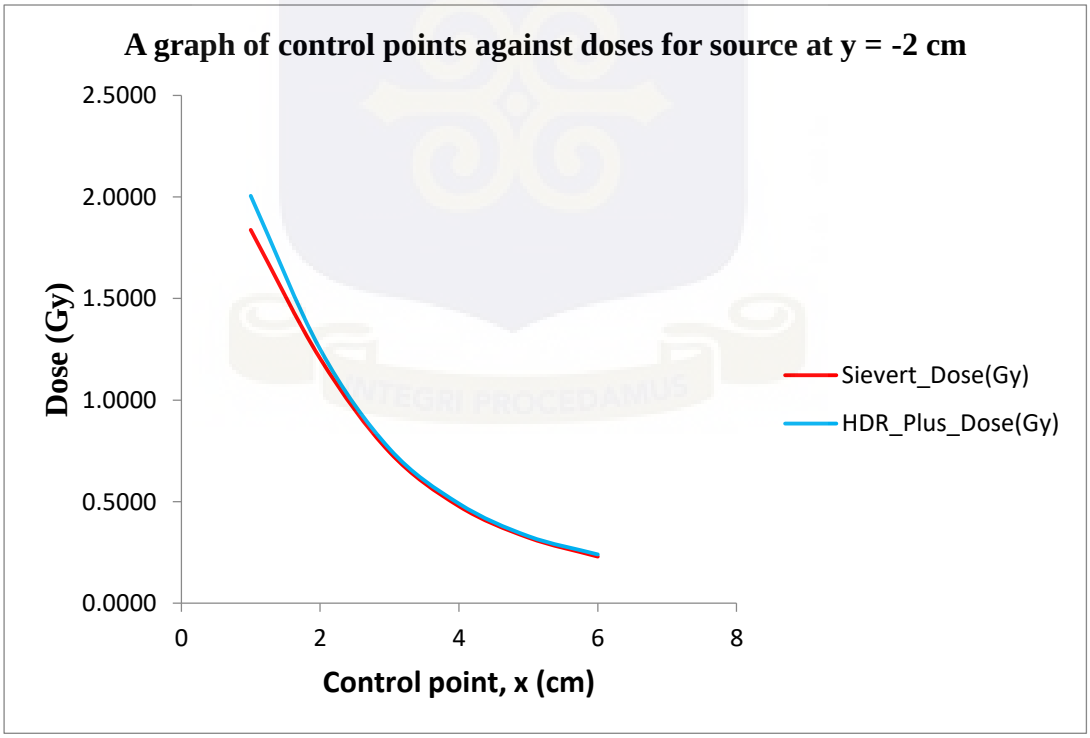

Figure 4. 13: Curves to compare dose outputs at y = -2cm

4.3 DISCUSSION

The observations made from the results obtained from the TPS clearly showed a general equality in dose values for points with the same distance and oblique directions from the source. However, this was not the case for the x = 1 cm control point (CP) readings for the source at the (0,-2), (0,-1), (0,1) and the (0,2) cm x-y co-ordinate location. The 100% mark to which the dose normalisation to x = 1 cm was done was only achieved for the scenario where the source was positioned at the perpendicular bisector or at the (0, 0) location, while a dose percentage of 99.5% and 99.6% of the prescribed 2 Gy was recorded for the (0,1) and (0,2) cm source dwell-positions respectively. When the source was positioned at the (0,-1) and (0,-2) cm

dwell-positions, the dose percentage, with respect to the 2 Gy prescribed, recorded was 100.5% and 100.4% respectively. These deviations from the expected outcome (100%) could be attributed to the influence of the encapsulation design as shown in figure 3.3. The non-uniformity in the distance from the core of the sealed source to the external part of the capsule could have resulted in the slight increase in the distance of the Co-60 source from the CP. Equality in the deviations for equidistant and equiangular points was expected but the greater thickness of the head of the capsule could have contributed to this variation and this resulted in the increment in the source dwell-time when the source was positioned below the perpendicular bisector. This is because the shielding of source was greater, hence a greater treatment time, 81.81 seconds for (0,-1) cm and 208.64 seconds for (0,-2) cm, was required to attain the prescribed dose as compared to the 78.68 seconds and 202.72 seconds used for the (0,1) cm and (0,2) cm respectively.

The Sievert integral technique, as stated earlier, was incapable of calculating the dose for the source positioned at (0,0) cm because the angle subtended with reference to the CPs was 0 degrees. However, it calculated the dose for all other source dwell positions, producing dose values that were in acceptable ranges in comparison to what was expected. Early approximations and rounding off of figures resulted in an increment in the error produced; hence the decision to work with figures with at least four places of decimal to increase the accuracy of produced results, and further reduces the percentage deviation. The simplicity and speed of the MATLAB program utilised in carrying out the calculations enabled the dose computations per control point to take an average period of 30 seconds. Also, the magnitude of x and y values were used in the computations to produce positive dose values (as a negative dose value would be meaningless); hence the dose value for CPs equidistant and equiangular from the source dwell-position were equal.

The general equality in the dose output at CPs equidistant and equiangular for both methods resulted in the use of the mean of the doses from each pair of points to compare and analyse the results. The dose outputs from both methods were generally close with less percentage deviation. It was observed that for extreme oblique directions, the percentage deviation of the Sievert integral dose output from the TG43 based HDRplus TPS was larger as compared to points of lesser angular value. This verifies what Williamson *et al* (1983) established, that the Sievert approach introduces significant errors and practically breaks down in the extreme oblique directions.

This is clearly shown from the variation in the heights of the bar charts in figures 4.6, 4.8, 4.10 and 4.12. The slightly large height difference between the bar for the x = 1 cm CP for the (0,2) cm and (0,-2) cm which represents a percentage deviation of 10.51% and 8.35% respectively.

In exception of very high deviations obtained from the extreme oblique directions, the Sievert integral dose output for the Co-60 has shown to be a reliable method to perform a quality control on the HDRplus TPS. This is evident in the overlap of the curves plotted for dose against distance for both methods, most especially for the (0,-1) cm source dwell-position.

The deviations recorded for the (0,-1) cm dwell-position had a range of 0.03 – 3.87% as compared to its counterpart, i.e. (0,1) cm dwell position with a range of 1.00 – 4.70% could be used to assume that the Sievert integral produces much accurate dose values with a higher treatment time. This could be confirmed with the range for the (0,2) cm and (0,-2) cm dwell position.

CHAPTER FIVE

CONCLUSION AND RECOMMENDATION

5.1 CONCLUSION

The model of the Sievert integral used in this research alongside the approximations applied, i.e. the Meisberger polynomial, has shown to be a valid model to calculate the dose distribution around the new BEBIG Co-60 except for the fact that extreme oblique directions need to be exempted in case it will be utilised for clinical QC procedures.

The percentage deviation range of the dose output from the Sievert integral in comparison to that of the output from the TPS is 0.03 – 10.51% with a mean of 3.13% for angle range of $0^{o} < \theta < 70^{o}$. The Sievert integral broke down at respectively large angles, which in this case was from above 60^{o}. Therefore, neglecting the breaking point, i.e. $\theta \geq 60^{o}$, the range becomes 0.03 – 5.63% with a mean value of 2.55% for the angle range of $0^{o} < \theta < 48^{o}$.

5.2 CLINICAL INTERPRETATION

Following the ICRU report 24 that the percentage deviation of dose values calculated should not exceed ±5% of the true value, the Sievert integral has proven to be a valid tool for quality control of the HDRplus using the range with less error. Also, for purposes of radiation protection and patient safety, the TG43 formalism has shown superiority because the Sievert integral required more exposure or treatment time to yield the expected dose in most cases.

5.3 RECOMMENDATION

5.3.1 FOR THE RESEARCH COMMUNITY

For further research, more CPs should be considered at points away from the horizontal axis, so as to observe for possible consistency in the correlation of the dose outputs between the two methods. This also has to be with source dwell positions equally positioned at points away from the vertical axis, for single and multiple sources as well.

The consistency that might be obtained could yield a factor that will be incorporated in the Sievert integral model implemented, for possible elimination of errors.

In addition to the variation in position of sources digitally, measurements should also be carried out in a medium of choice so that three set of outputs would be obtained for a much more comprehensive analysis of the outcomes.

5.3.2 FOR THE CLINICAL COMMUNITY

It should be ensured that points located equidistant and equiangular from the source should receive equal dose during treatment through ensuring that the source encapsulation is uniform radially.

The Sievert integral has proven to be quite an accurate tool for calculation of dose around a Co-60 source just as established for Ir-192, it will therefore be recommended that a facility using the new Bebig Co-60 source would consider implementing the model of the Sievert integral used for this research to carryout quality control procedures on their HDRplus TPS.

REFERENCES

Acquah G. F., (2011). Fitting And Benchmarking Of Monte Carlo Output Parameters For Ir-192 High Dose Rate Brachytherapy Source (MPhil Thesis). University of Ghana, Accra, Ghana.

Baltas, D., Karaiskos, P., Papagiannis, P., Sakelliou, L., Loeffler E., and Zamboglou N. (2001) Beta versus gamma dosimetry close to Ir-192 brachytherapy sources, Med. Phys., 28:1875,.

Baltas D., Zamboglou N., Sakelliou L., (2007) The Physics of Modern Brachytherapy For Oncology; Series in Medical Physics and Biomedical Engineering; CRC Press Taylor & Francis Group 6000 Broken Sound Parkway NW, pp 393-396.

Bhola S. *et al* (2012) An analytic approach to the dosimetry of a new BEBIG Co-60 HDR Brachytherapy Source, Journal of Medical Physics, doi: 10.4103/0971-620399228, India

Cohen G. N., Amols H. I., Zaider M. (2000) An independent dose-to point calculation program for the verification of high-dose-rate brachytherapy treatment planning. Int J Radiation Oncology Biology & Physics; 48:1251–1258.

Daskalov G. M., Loffler E., Williamson J. F. (1998), Monte Carlo–aided dosimetry of a new high dose-rate brachytherapy source. Journal of Medical Physics; 1998; 25:2200–2208.

Hahn B. D., Valentine D. T.,(2007) Essential MATLAB for Engineers and Scientists (3rd Edition), Elsevier Ltd, Oxford, U. K.

International Atomic Energy Agency (IAEA) textbook (2007) "Radiation oncology physics: a handbook for teachers and students", chapter 13, Brachytherapy: physical and clinical aspects. 373-375.

Interstitial Collaborative Working Group (ICWG) (1990); Interstitial Brachytherapy Physical, Biological and Clinical Considerations. Edited by Anderson L. L., Nath R. and Weaver K. A. Raven – New York,

International Commission on Radiation Units and Measurements, (1997) Dose and volume specification for reporting interstitial therapy, ICRU Report 58.ICRU, Bethesda.

Karaiskos P., Papagiannis P., Sakelliou L., Anagnostopoulos A., and Baltas D., (2001) Monte Carlo dosimetry of the select Seed ^{125}I interstitial brachytherapy seed, Med. Phys., 28, pp 1753

Kemmerer T., Lahanas M., Baltas D., Zamboglou N., (2000) DVH Computation Comparisons Using Conventional Methods And Optimized Fast Fourier Transform Algorithm For Brachytherapy; Journal of Medical Physics

Khan, F. M., (1994) Brachytherapy In: "The physics in radiation therapy "(William M. P. ed), 2nd edition, pp 418-473. Williams & Wilkins, Baltimore, U.S.A.

Khan F. M., (2010), The Physics of Radiation Therapy, Philadelphia (4th Edition), Lippincott Williams & Wilkins, Philadelphia, U.S.A.

Kline R. W., Earle J. D. (2007) Implementation of TG43 for dose prescription and calculation of ^{192}Ir Eye Plaques; Mayo Clinic, Rochester, MN update 9

Kyeremeh P. O., (2011). Three Dimensional Implementation of Anisotropy Corrected Fast Fourier Transform Dose Calculation Around Brachytherapy Seeds (MPhil Thesis). University of Ghana, Accra, Ghana.

Kyeremeh P.O., Nani E.K., Addison E.K.T., Hasford F., (2012) Implementation of 3DAnisotropy Corrected Fast Fourier Transform Dose Calculation around Brachytherapy Seeds, International Journal of Science and Technology Volume 2 No.3, ISSN 2224-3577

Ling C. C. *et al*: (1985) Two-Dimensional dose distribution of ^{125}I, Journal of Medical Physics, 1985: 12:652-655

Lu L., (2013) Dose Calculation Algorithms in External Beam Photon Radiation Therapy, International Journal of Cancer Therapy & Oncology; 1(2):01025. DOI: 10.14319/ijcto.0102.5

Meli J. A., Meigooni A. S., Narth R., (1988) On The Choice of phantom materials for the dosimetry of Ir-192 sources. International Journal for radiation oncology, biology and physics; 14:586-595.

Meredith W.J, ed. (1947), The Manchester System, Livingstone, Edinburgh.

Miften M., Wiesmeyer M., Monthofer S., *et al*, (1999) Implementation of FFT Convolution and Multigrid Superposition Models In The FOCUS RTP System, Physics, Medicine & Biology Journal; 45:817-833

Nani E.K., Akaho E.H.K., Kyere A.W.K., Amuasi J.H. *et al* (2009); Approximating Sievert Integrals to Monte Carlo methods to calculate dose rate distributions around Ir-192 brachytherapy source, Journal of Applied Science & Technology, Vol. 14, page 27-31.

Nath R, Anderson L, Luxton G, Weaver A, Williamson F, Meigooni S. (1995) Dosimetry of interstitial brachytherapy sources Recommendations of the AAPM Radiation Therapy Committee Task Group 43. Med Phys.; 22:209-34 [PubMed]

Nath R, Park C H, King C R and Muench P (1990) A dose computation model for 241Am vaginal applicators including the source-to-source shielding effects Med. Phys. 17 833–42

Neuenschwander H., Machie T. R., Reckwerdt P. J. (1995); MMC-A High Performance Monte Carlo Code For Electron Beam Treatment Planning. Physics, Medicine & Biology Journal; 40:543-574

Oelke U., Scholz C., (2006). New Technologies In Radiation Oncology, Medical Radiology, Part 3, pp 187-196, DOI: 10:1007/3-540-29999-8_15

Oguchi H. *et al* (2005). Advantage of Multiple Algorithm In Treatment Planning System For External Beam Dose Calculation

Pantelis E., Baltas D, Dardoufas K, *et al*, (2002) On the accuracy of the Sievert Integral Model in the proximity of Ir-192 HDR sources, Int J. Radiation oncology Biol. Phys, Vol 53, No 4, pp 1071-1084

Papanikolaou N., Battista J. J., Boyer A. L., Kappas C., Klein E., *et al* (2004) Tissue Inhomogeneity Correction For Megavoltage Photon Beams, An AAPM Report No. 85, Report of task group No. 65 of the radiation therapy committee of AAPM, pp 47-64

Papanikolaou N., Stathakis S., (2009), Dose Calculation Algorithms In Context of Inhomogenous Correction For High Energy Photon Beams, Department of Radiation Oncology , Cancer Therapy and Research Center , University of Texas Health Sciences Center, San Antonnio, Texas 78229, USA,36(10):4765-75

Podgorsak E.B., (2005). Radiation Oncology Physics: A Handbook For Teachers And Students, International Atomic Energy Agency, Vienna, Austria

Quimby, E.H. (1922) The effect of the size of radium applicators on skin doses, Am. J. Roentgenol., 9, 671 – 683.

Ravinder N., *et al*, (1994) dosimetry of interstial brachytherapy sources: recommendations of the AAPM radiation therapy Committee Task Group No.43, Journal of Medical Physics; 22:; 210

Rivard J, Coursey M, Dewerd A, Hanson F, Huq S, Ibbott S, *et al*. (2004) Update of AAPM Task Grooup 43 Report: A revised AAPM protocol for brachytherapy dose calculations. Med Phys.; 31:633-744. [PubMed]

Schell M. C., Ling C. C., Gromadzki Z. C., Working K. R. (1987); Dose distribution of model 6702 ^{125}I seeds in water; International Journal of Radiation Oncology, Biology and Physics:13; 795-799

Sievert, R. (1921) Die Intensita¨ tsverteilung der primaeren Gammastrahlung in der Naehe medizinscher Radiumpra¨parate, Acta. Radiol., 1, 89 – 128.

Sievert Integral, http://en.wikipedia.org/wiki/Sievert_integral.html [18th March, 2017]

Wang, R. and Li, X.A. (2000) A Monte Carlo Calculation Of Dosimetric Parameters Of 90Sr/90Y And 192Ir SS Sources For Intravascular Brachytherapy, Med. Phys., 27, 2528

Weaver K. (1998) Anisotropy functions for ^{125}I and ^{103}Pd sources, Med. Phys., 25, 2271.

Weaver K. A., *et al*, (1989) Dose Parameters of ^{125}I and ^{192}Ir seed sources, Journal of Medical Physics, 16:636-643

Wickham, L. and Degrais, P. (1910) Radiumtherapy, English ed., Cassell, London,.

Williamson, J.F., Coursey, B.M., DeWerd, L.A., Hanson, W.F., and Meigooni, A.S. (1998) Dosimetric Prerequisites For Routine Clinical Use Of New Low Energy Photon Interstitial Brachytherapy Sources, Med. Phys., 25, 2269,.

Williamson J. F., Morin R.L., Khan F. M. (1983) Monte Carlo evaluation of Sievert integral for brachytherapy dosimetry. Phys Med Biol. 28:1021

Williamson J. F., (1996) The Sievert integral revisited: Evaluation and extension to I-125, Yb-169, and Ir-192 brachytherapy sources, Int. Journal of radiation oncology Biol Phys 36:1239-1250

World Health Rankings; *Health Profile: Ghana*, *http://www.worldlifeexpectancy.com/country-health-profile/ghana.html*, [12th January, 2017]

APPENDICES

APPENDIX A: Dose Control Point Report for source at y = 0 cm

Dwell Position Report

Applicator <1>: LLA1200-20

Dwell-Index	from Tip [cm]	X-Pos [cm]	Y-Pos [cm]	Z-Pos [cm]	Dwell-Time [s]
7	3.48	0.00	-0.01	0.02	40.25

Total Dwell Time for this Applicator : 40.25 s = 00:00:40

Total Dwell Time for this Study: 40.25 s = 00:00:40

Total Reference Air Kerma (TRAK) : 0.01827 cGy·m²

Dose Control Point Report

Rx = 2.00 Gy

Ctrl Point Group Name: MP

Min. Dose: 0.05 Gy; Average Dose: 0.49 Gy (24.63% Rx); Max. Dose: 2.00 Gy;

Idx	Name	X-Pos [cm]	Y-Pos [cm]	Z-Pos [cm]	Dose [Gy]	Dose % Rx
1		-6.00	0.00	0.00	0.05	2.6
2		-5.00	0.00	0.00	0.08	3.8
3		-4.00	0.00	0.00	0.12	6.0
4		-3.00	0.00	0.00	0.22	10.8
5		-2.00	0.00	0.00	0.49	24.7
6		-1.00	0.00	0.00	2.00	100.0
7		1.00	0.00	0.00	2.00	100.0
8		2.00	0.00	0.00	0.49	24.7
9		3.00	0.00	0.00	0.22	10.8
10		4.00	0.00	0.00	0.12	6.0
11		5.00	0.00	0.00	0.07	3.7
12		6.00	0.00	0.00	0.05	2.6

Ctrl Point Group Name: NORM

Min. Dose: 2782.91 Gy; Average Dose: 2782.91 Gy (139145.40% Rx); Max. Dose: 2782.91 Gy;

Idx	Name	X-Pos [cm]	Y-Pos [cm]	Z-Pos [cm]	Dose [Gy]	Dose % Rx
1		0.00	0.00	0.00	2,782.91	139,145.4

APPENDIX B: Dose Control Point Report for source at y = 1 cm

Dwell Position Report

Applicator <1>: LLA1200-20

Dwell-Index	from Tip [cm]	X-Pos [cm]	Y-Pos [cm]	Z-Pos [cm]	Dwell-Time [s]
5	2.48	0.00	0.00	-0.98	78.68

Total Dwell Time for this Applicator : 78.68 s = 00:01:19

Total Dwell Time for this Study: 78.68 s = 00:01:19

Total Reference Air Kerma (TRAK) : 0.03572 cGy·m²

Dose Control Point Report

Rx = 2.00 Gy

Ctrl Point Group Name: MP

Min. Dose: 0.10 Gy; Average Dose: 0.60 Gy (30.08% Rx); Max. Dose: 2.00 Gy;

Idx	Name	X-Pos [cm]	Y-Pos [cm]	Z-Pos [cm]	Dose [Gy]	Dose % Rx
1		-6.00	0.00	0.00	0.10	4.9
2		-5.00	0.00	0.00	0.14	7.1
3		-4.00	0.00	0.00	0.22	11.0
4		-3.00	0.00	0.00	0.38	19.0
5		-2.00	0.00	0.00	0.78	38.8
6		-1.00	0.00	0.00	2.00	100.0
7		1.00	0.00	0.00	1.99	99.5
8		2.00	0.00	0.00	0.78	38.8
9		3.00	0.00	0.00	0.38	19.0
10		4.00	0.00	0.00	0.22	11.0
11		5.00	0.00	0.00	0.14	7.0
12		6.00	0.00	0.00	0.10	4.9

APPENDIX C: Isodose report for source at y = 1cm

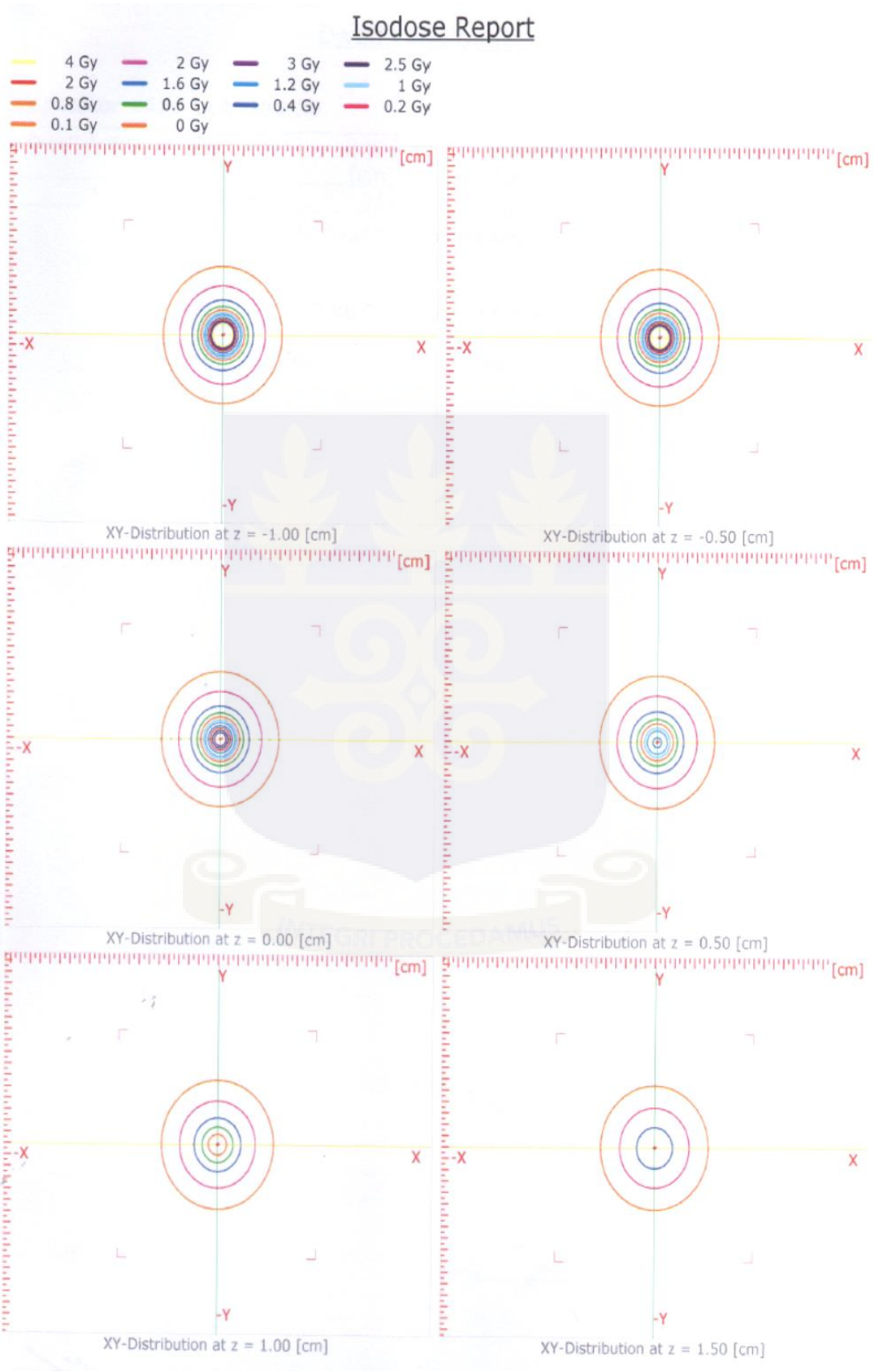

APPENDIX D: Dose Control Point Report for source at y = 2 cm

Dwell Position Report

Applicator <1>: LLA1200-20

Dwell-Index	from Tip [cm]	X-Pos [cm]	Y-Pos [cm]	Z-Pos [cm]	Dwell-Time [s]
3	1.48	0.00	0.00	-1.98	202.72

Total Dwell Time for this Applicator : 202.72 s = 00:03:23

Total Dwell Time for this Study: 202.72 s = 00:03:23

Total Reference Air Kerma (TRAK) : 0.09203 cGy·m²

Dose Control Point Report

Rx = 2.00 Gy

Ctrl Point Group Name: MP

Min. Dose: 0.23 Gy; Average Dose: 0.84 Gy (41.80% Rx); Max. Dose: 2.00 Gy;

Idx	Name	X-Pos [cm]	Y-Pos [cm]	Z-Pos [cm]	Dose [Gy]	Dose % Rx
1		-6.00	0.00	0.00	0.23	11.6
2		-5.00	0.00	0.00	0.32	16.2
3		-4.00	0.00	0.00	0.48	23.9
4		-3.00	0.00	0.00	0.75	37.5
5		-2.00	0.00	0.00	1.24	61.9
6		-1.00	0.00	0.00	2.00	100.0
7		1.00	0.00	0.00	1.99	99.6
8		2.00	0.00	0.00	1.24	61.9
9		3.00	0.00	0.00	0.75	37.4
10		4.00	0.00	0.00	0.48	23.9
11		5.00	0.00	0.00	0.32	16.2
12		6.00	0.00	0.00	0.23	11.5

APPENDIX E: Isodose Report for source at y = 2 cm

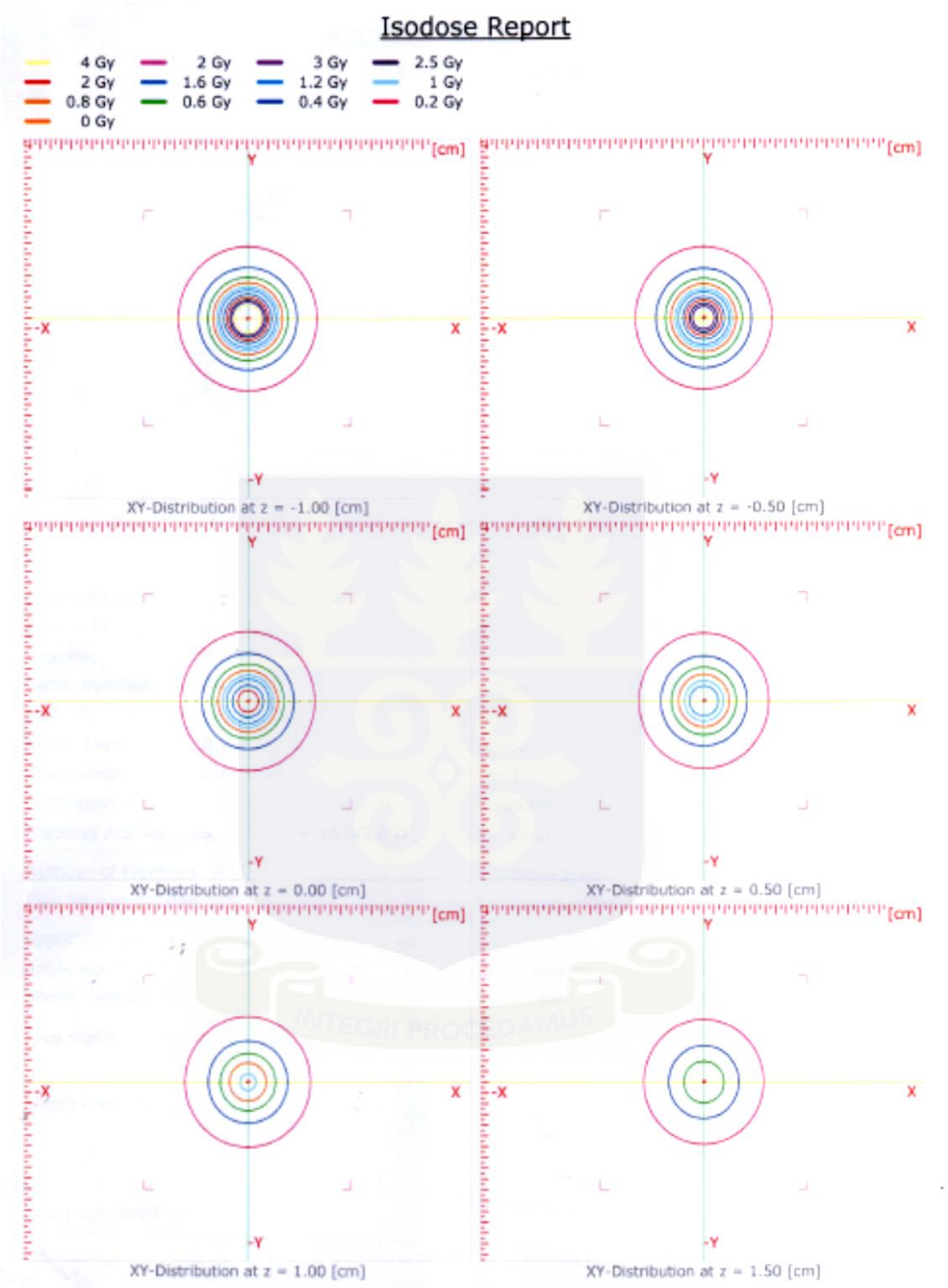

APPENDIX F: Dose Control point Report for source at y = -1 cm

Dwell Position Report

Applicator <1>: LLA1200-20

Dwell-Index	from Tip [cm]	X-Pos [cm]	Y-Pos [cm]	Z-Pos [cm]	Dwell-Time [s]
9	4.48	0.00	-0.01	1.02	81.81

Total Dwell Time for this Applicator : 81.81 s = 00:01:22

Total Dwell Time for this Study: 81.81 s = 00:01:22

Total Reference Air Kerma (TRAK) : 0.03714 cGy·m²

Dose Control Point Report

Rx = 2.00 Gy

Ctrl Point Group Name: MP

Min. Dose: 0.10 Gy; Average Dose: 0.61 Gy (30.55% Rx); Max. Dose: 2.01 Gy;

Idx	Name	X-Pos [cm]	Y-Pos [cm]	Z-Pos [cm]	Dose [Gy]	Dose % Rx
1		-6.00	0.00	0.00	0.10	5.0
2		-5.00	0.00	0.00	0.15	7.3
3		-4.00	0.00	0.00	0.23	11.4
4		-3.00	0.00	0.00	0.39	19.6
5		-2.00	0.00	0.00	0.79	39.7
6		-1.00	0.00	0.00	2.00	100.0
7		1.00	0.00	0.00	2.01	100.5
8		2.00	0.00	0.00	0.79	39.7
9		3.00	0.00	0.00	0.39	19.6
10		4.00	0.00	0.00	0.23	11.4
11		5.00	0.00	0.00	0.15	7.3
12		6.00	0.00	0.00	0.10	5.1

APPENDIX G: Isodose Report for source at y = -1 cm

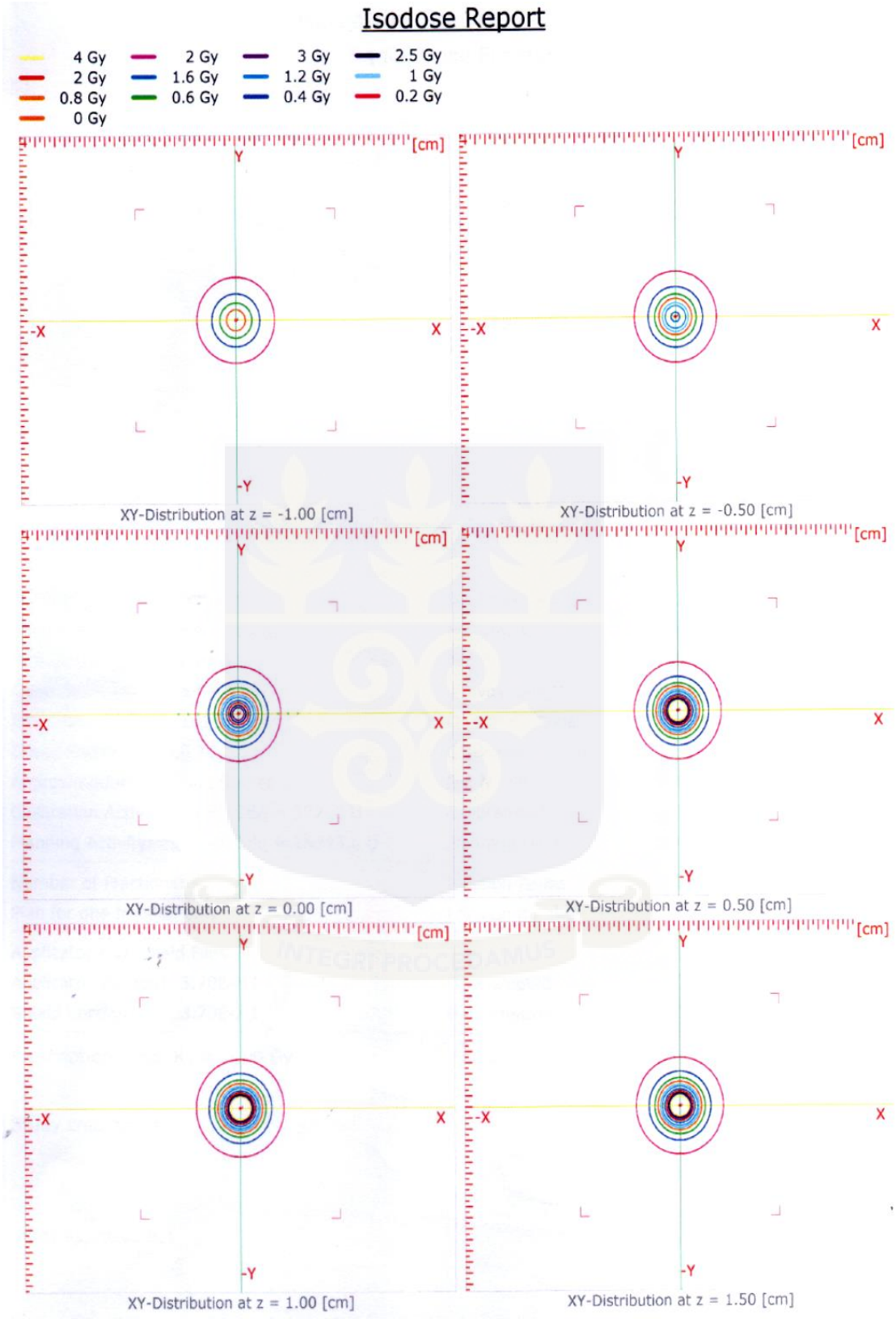

APPENDIX H: Dose control point Report for source at y = -2 cm

Dwell Position Report

Applicator <1>: LLA1200-20

Dwell-Index	from Tip [cm]	X-Pos [cm]	Y-Pos [cm]	Z-Pos [cm]	Dwell-Time [s]
11	5.48	0.00	-0.01	2.02	208.64

Total Dwell Time for this Applicator : 208.64 s = 00:03:29

Total Dwell Time for this Study: 208.64 s = 00:03:29

Total Reference Air Kerma (TRAK) : 0.09472 cGy·m²

Dose Control Point Report

Rx = 2.00 Gy

Ctrl Point Group Name: MP

Min. Dose: 0.24 Gy; Average Dose: 0.85 Gy (42.26% Rx); Max. Dose: 2.01 Gy;

Idx	Name	X-Pos [cm]	Y-Pos [cm]	Z-Pos [cm]	Dose [Gy]	Dose % Rx
1		-6.00	0.00	0.00	0.24	11.8
2		-5.00	0.00	0.00	0.33	16.6
3		-4.00	0.00	0.00	0.49	24.4
4		-3.00	0.00	0.00	0.76	38.1
5		-2.00	0.00	0.00	1.25	62.5
6		-1.00	0.00	0.00	2.00	100.0
7		1.00	0.00	0.00	2.01	100.4
8		2.00	0.00	0.00	1.25	62.5
9		3.00	0.00	0.00	0.76	38.0
10		4.00	0.00	0.00	0.49	24.4
11		5.00	0.00	0.00	0.33	16.6
12		6.00	0.00	0.00	0.24	11.9

APPENDIX I: Isodose Report for source at y = -2 cm

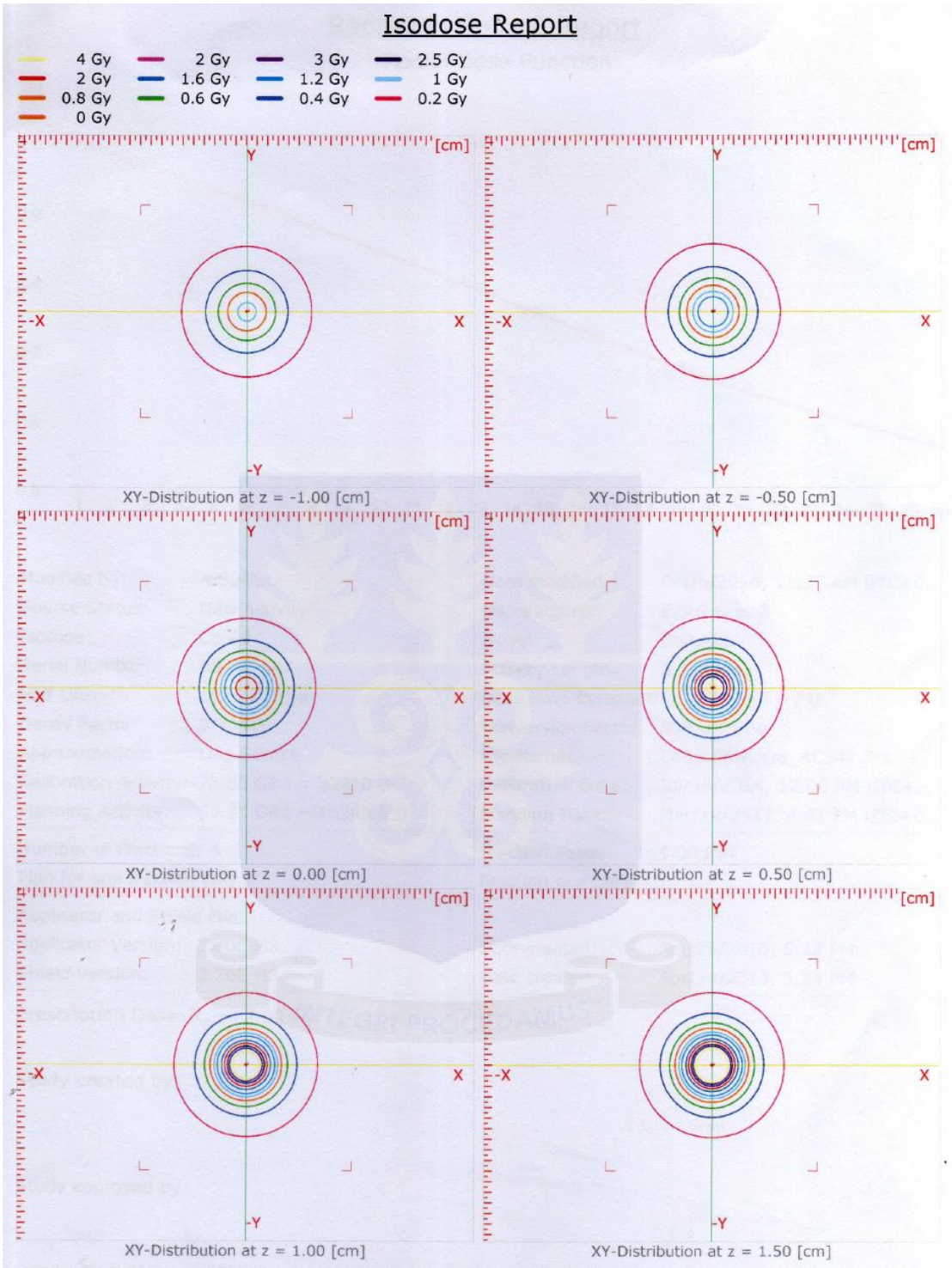

APPENDIX J: The New BEBIG Co-60 HDR Source Details

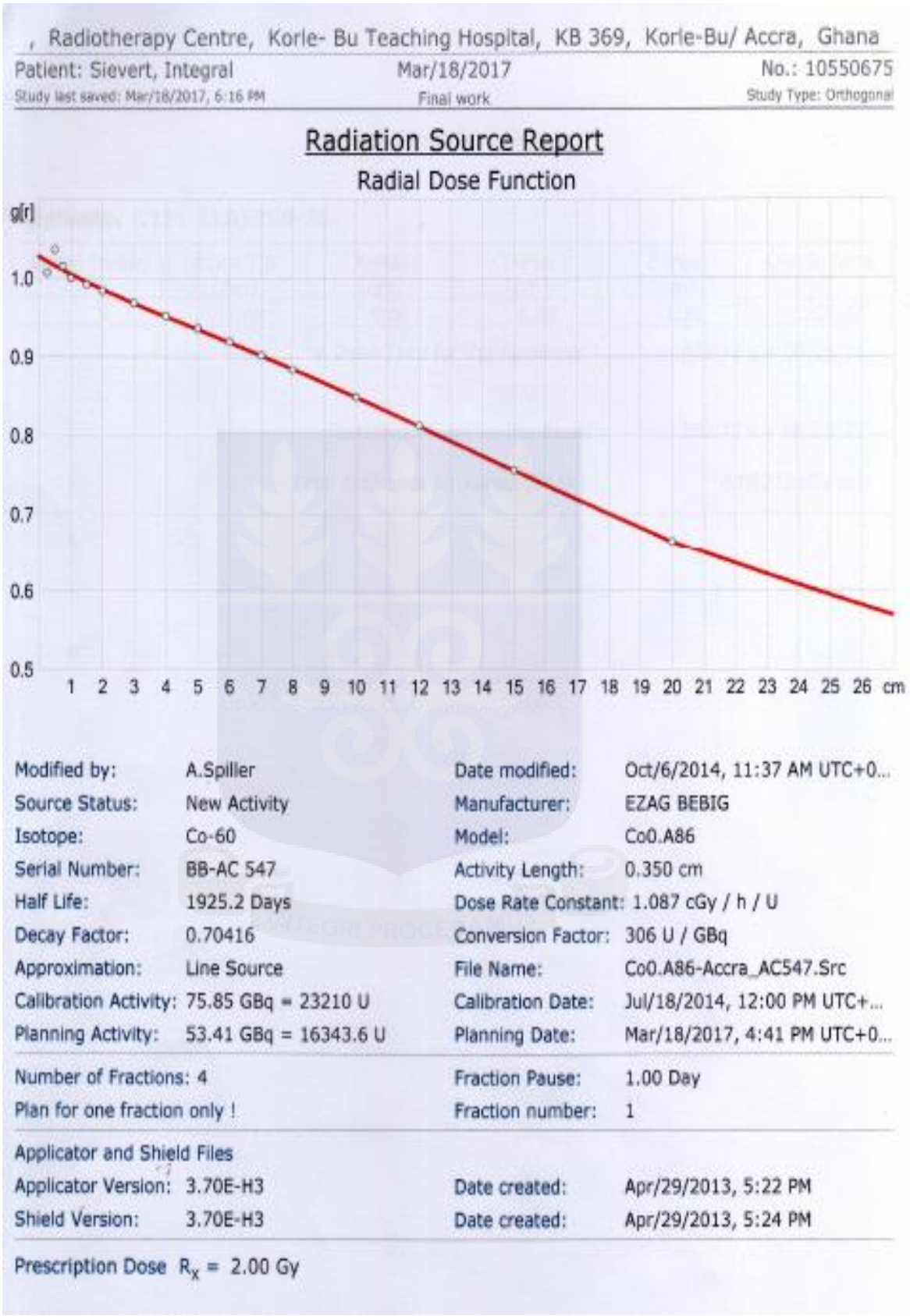

APPENDIX K: MATLAB SYNTAX

```
% This program calculates the dose distribution around
the High Dose Rate
% (HDR) Multisource Afterloader of the New Bebig Machine
% Source: Cobalt-6o
% Number of control points (points of measurement): 12
% Number of source positions: 5
% y = (-2, -1, 0, +1, +2)
% Parameters used and their corresponding units are:
% D = Dose (Gy)
% Sk = Air Kerma Strength (cGy.cm^2.h^-1)
% L = active source length (m)
% y = source posoition (cm)
% mu = effective attenuation coefficient (cm^-1)
% t = wall thickness (cm)
% x = control point (cm)
% t_dwell = dwell time (seconds)
% W/e = average enrgy per unit charge (cGy.kg/C)
% fmed = roentgen-to-rad conversion factor or f factor
(Gy.kg/C)
% SIV = Sievert Integral value for each angle
% SPR = scatter-to-primary ratio
clear all
close all
clc
x = input('Enter the value of x: ')

y1 = input('Enter the value of y1: ')
y2 = input('Enter the value of y2: ')

r1 = sqrt((x^2)+(y1^2));
r2 = sqrt((x^2)+(y2^2));

SIV1 = input('Enter the Sievert Integral Value for y1: ')
SIV2 = input('Enter the Sievert Integral Value for y2: ')
t_dwell = input ('Enter the source dwell time: ')
time = t_dwell/3600;

A = 0.99423; B = -0.005318;
C = -0.002610; D = 0.0001327;
j = exp(mu*t);
num = fmed*Sk*time*j;
den = L*x*We;
D1 = (num/den)*SIV1*SPR1
D2 = (num/den)*SIV2*SPR2
Doses = [D1 D2]
diff = D2-D1
```

APPENDIX L: General Sievert Integral Table

Sievert Integral $\int_0^{\theta} e^{-x \sec \phi} d\phi$ **Table 27.4**

$x \backslash \theta$	10°	20°	30°	40°	50°	60°	75°	90°
0.0	0.174533	0.349066	0.523599	0.698132	0.872665	1.047198	1.308997	1.570796
0.1	0.157843	0.315187	0.471456	0.625886	0.777323	0.923778	1.123611	1.228632
0.2	0.142749	0.284598	0.424515	0.561159	0.692565	0.815477	0.968414	1.023680
0.3	0.129099	0.256978	0.382255	0.503165	0.617194	0.720366	0.837712	0.868832
0.4	0.116754	0.232040	0.344209	0.451198	0.550154	0.636769	0.727031	0.745203
0.5	0.105589	0.209522	0.309957	0.404629	0.490508	0.563236	0.632830	0.643694
0.6	0.095492	0.189191	0.279118	0.362893	0.437428	0.498504	0.552287	0.558890
0.7	0.086361	0.170833	0.251353	0.325486	0.390178	0.441478	0.483134	0.487198
0.8	0.078103	0.154256	0.226354	0.291957	0.348109	0.391204	0.423535	0.426062
0.9	0.070634	0.139289	0.203845	0.261901	0.310642	0.346851	0.371996	0.373579
1.0	0.063880	0.125775	0.183579	0.234956	0.277267	0.307694	0.327288	0.328286
1.2	0.052247	0.102553	0.148899	0.189138	0.221027	0.242523	0.254485	0.254889
1.4	0.042733	0.083620	0.120780	0.152298	0.176336	0.191533	0.198885	0.199051
1.6	0.034951	0.068183	0.097979	0.122667	0.140792	0.151541	0.156087	0.156156
1.8	0.028587	0.055597	0.079488	0.098829	0.112497	0.120105	0.122932	0.122961
2.0	0.023381	0.045335	0.064492	0.079644	0.089954	0.095342	0.097108	0.097121
2.2	0.019123	0.036967	0.052329	0.064201	0.071979	0.075797	0.076905	0.076911
2.4	0.015641	0.030145	0.042463	0.051766	0.057635	0.060342	0.061040	0.061043
2.6	0.012793	0.024582	0.034460	0.041750	0.046179	0.048100	0.048541	0.048542
2.8	0.010463	0.020045	0.027968	0.033680	0.037024	0.038387	0.038667	0.038668
3.0	0.008558	0.016347	0.022700	0.027177	0.029702	0.030670	0.030848	0.030848
3.5	0.005178	0.009817	0.013477	0.015912	0.017164	0.017576	0.017634	0.017634
4.0	0.003132	0.005896	0.008005	0.009330	0.009951	0.010128	0.010147	0.010147
4.5	0.001895	0.003542	0.004756	0.005478	0.005787	0.005862	0.005869	0.005869
5.0	0.001147	0.002127	0.002828	0.003221	0.003374	0.003407	0.003409	0.003409
5.5	0.000694	0.001278	0.001682	0.001896	0.001972	0.001986	0.001987	0.001987
6.0	0.000420	0.000768	0.001001	0.001117	0.001155	0.001162	0.001162	0.001162
6.5	0.000254	0.000461	0.000596	0.000659	0.000678	0.000681	0.000681	0.000681
7.0	0.000154	0.000277	0.000355	0.000389	0.000399	0.000400	0.000400	0.000400
7.5	0.000093	0.000167	0.000211	0.000230	0.000235	0.000235	0.000235	0.000235
8.0	0.000056	0.000100	0.000126	0.000136	0.000139	0.000139	0.000139	0.000139
8.5	0.000034	0.000060	0.000075	0.000081	0.000082	0.000082	0.000082	0.000082
9.0	0.000021	0.000036	0.000045	0.000048	0.000048	0.000048	0.000048	0.000048
9.5	0.000012	0.000022	0.000027	0.000028	0.000029	0.000029	0.000029	0.000029
10.0	0.000008	0.000013	0.000016	0.000017	0.000017	0.000017	0.000017	0.000017

APPENDIX M: Sievert Integral Table for angles of CPs

Sievert Integral Values for θ									
x/θ	9.46	11.31	14.04	18.43	21.8	26.57	33.69	45	63.43
0.125	0.16314	0.19503	0.24209	0.31777	0.37539	0.458	0.58083	0.77579	1.08986

Sievert Integral Values for θ1												
x/θ1	7.83	9.37	11.65	15.38	16.92	20.05	22.42	24.52	31.31	39.52	42.38	61.28
0.125	0.13504	0.16159	0.20089	0.26519	0.29174	0.34569	0.38652	0.42269	0.53968	0.68228	0.73125	1.05345

Sievert Integral Values for θ2												
x/θ2	11.08	13.22	16.37	19.93	21.39	23.51	28.54	30.43	35.94	47.4	49.6	65.31
0.125	0.19106	0.22796	0.28226	0.34362	0.36877	0.40529	0.49193	0.5245	0.61953	0.81719	0.854	1.12108

APPENDIX N: Dose Control Point Report as computed using the Sievert integral for source at y = 1cm

x (cm)	y (cm)	y1 (cm)	y2 (cm)	θ (deg)	θ1 (deg)	θ2 (deg)	SIV1	SIV2	D1(Gy)	D2(Gy)	Sievert_Dose(Gy)
1	1	0.825	1.175	45.00	39.52	49.60	0.682276	0.853998	7.6771	9.5807	1.9036
2	1	0.825	1.175	26.57	22.42	30.43	0.386516	0.524497	2.1494	2.909700	0.7603
3	1	0.825	1.175	18.43	15.38	21.39	0.265190	0.368774	0.9675	1.3427	0.3752
4	1	0.825	1.175	14.04	11.65	16.37	0.200890	0.282256	0.5391	0.7561	0.2170
5	1	0.825	1.175	11.31	9.37	13.22	0.161587	0.227955	0.3393	0.4779	0.1386
6	1	0.825	1.175	9.46	7.83	11.08	0.135040	0.191064	0.2307	0.326	0.0953

APPENDIX O: Dose Control Point Report as computed using the Sievert integral for source at y = 2 cm

x (cm)	y (cm)	y1 (cm)	y2 (cm)	θ (deg)	θ1 (deg)	θ2 (deg)	SIV1	SIV2	D1(Gy)	D2(Gy)	Sievert_Dose(Gy)
1	2	1.825	2.175	63.43	61.28	65.31	1.053450	1.121084	30.2248	32.0102	1.7854
2	2	1.825	2.175	45.00	42.38	47.40	0.731250	0.817187	10.3854	11.5556	1.1702
3	2	1.825	2.175	33.69	31.31	35.94	0.539675	0.619531	5.0344	5.7569	0.7225
4	2	1.825	2.175	26.57	24.52	28.54	0.422688	0.491933	2.9029	3.3667	0.4638
5	2	1.825	2.175	21.80	20.05	23.51	0.345692	0.405291	1.8592	2.1729	0.3137
6	2	1.825	2.175	18.43	16.92	19.93	0.291737	0.343624	1.2773	1.5003	0.223

APPENDIX P: Dose Control Point Report as computed using the Sievert integral for source at y = -1 cm

x (cm)	y (cm)	y1 (cm)	y2 (cm)	θ (deg)	θ1 (deg)	θ2 (deg)	SIV1	SIV2	D1(Gy)	D2(Gy)	Sievert_Dose(Gy)
1	-1	0.825	1.175	45.00	39.52	49.60	0.682276	0.853998	7.9825	9.9618	1.9793
2	-1	0.825	1.175	26.57	22.42	30.43	0.386516	0.524497	2.2349	3.0254	0.7905
3	-1	0.825	1.175	18.43	15.38	21.39	0.265190	0.368774	1.0060	1.3961	0.3901
4	-1	0.825	1.175	14.04	11.65	16.37	0.200890	0.282256	0.5606	0.7862	0.2256
5	-1	0.825	1.175	11.31	9.37	13.22	0.161587	0.227955	0.3528	0.497	0.1442
6	-1	0.825	1.175	9.46	7.83	11.08	0.135040	0.191064	0.2399	0.3389	0.0990

APPENDIX Q: Dose Control Point Report as computed using the Sievert integral for source at y = -2 cm

x (cm)	y (cm)	y1 (cm)	y2 (cm)	θ (deg)	θ1 (deg)	θ2 (deg)	SIV1	SIV2	D1(Gy)	D2(Gy)	Sievert_Dose(Gy)
1	-2	1.825	2.175	63.43	61.28	65.31	1.053450	1.121084	31.1075	32.945	1.8375
2	-2	1.825	2.175	45.00	42.38	47.40	0.731250	0.817187	10.6887	11.893	1.2043
3	-2	1.825	2.175	33.69	31.31	35.94	0.539675	0.619531	5.1814	5.925	0.7436
4	-2	1.825	2.175	26.57	24.52	28.54	0.422688	0.491933	2.9877	3.4651	0.4774
5	-2	1.825	2.175	21.80	20.05	23.51	0.345692	0.405291	1.9135	2.2364	0.3229
6	-2	1.825	2.175	18.43	16.92	19.93	0.291737	0.343624	1.3147	1.5442	0.2295